Environment International 185 (2024) 108553

Contents lists available at ScienceDirect

Environment International

journal homepage: www.elsevier.com/locate/envint

Full length article

Recommendations for reporting equivalent black carbon (eBC) mass concentrations based on long-term pan-European in-situ observations

Marjan Savadkoohi [a,b,*], Marco Pandolfi [a,*], Olivier Favez [c], Jean-Philippe Putaud [d], Konstantinos Eleftheriadis [e], Markus Fiebig [f], Philip K. Hopke [g,h], Paolo Laj [i], Alfred Wiedensohler [j], Lucas Alados-Arboledas [k], Susanne Bastian [l], Benjamin Chazeau [m,n], Álvaro Clemente María [o], Cristina Colombi [p], Francesca Costabile [q], David C. Green [r,s], Christoph Hueglin [t], Eleni Liakakou [u], Krista Luoma [v], Stefano Listrani [w], Nikos Mihalopoulos [u], Nicolas Marchand [m], Griša Močnik [x,y], Jarkko V. Niemi [z], Jakub Ondráček [aa], Jean-Eudes Petit [ab], Oliver V. Rattigan [ac], Cristina Reche [a], Hilkka Timonen [v], Gloria Titos [k], Anja H. Tremper [r], Stergios Vratolis [e], Petr Vodička [aa], Eduardo Yubero Funes [o], Naděžda Zíková [aa], Roy M. Harrison [ad,ae], Tuukka Petäjä [af], Andrés Alastuey [a], Xavier Querol [a]

[a] *Institute of Environmental Assessment and Water Research (IDAEA-CSIC), Barcelona, Spain*
[b] *Department of Natural Resources & Environment, Industrial & TIC Engineering (EMIT-UPC), Manresa, Spain*
[c] *Institut National de l'Environnement Industriel et des Risques (INERIS), Verneuil-en-Halatte, France*
[d] *European Commission, Joint Research Centre (JRC), Ispra, Italy*
[e] *Environmental Radioactivity & Aerosol Technology for Atmospheric & Climate Impact Lab, INRaSTES, NCSR "Demokritos", Athens, Greece*
[f] *Dept. Atmospheric and Climate Research, NILU-Norwegian Institute for Air Research, Kjeller, Norway*
[g] *Department of Public Health Sciences, University of Rochester School of Medicine & Dentistry, Rochester, NY, USA*
[h] *Institute for a Sustainable Environment, Clarkson University, Potsdam, NY, USA*
[i] *Univ. Grenoble, CNRS, IRD, IGE, 38000 Grenoble, France*
[j] *Leibniz Institute for Tropospheric Research (TROPOS), Leipzig, Germany*
[k] *Andalusian Institute for Earth System Research (IISTA-CEAMA), University of Granada, Granada, Spain*
[l] *Saxon State Office for Environment, Agriculture and Geology/Saxon State Department for Agricultural and Environmental Operations, Dresden, Germany*
[m] *Aix Marseille Univ., CNRS, LCE, Marseille, France*
[n] *Laboratory of Atmospheric Chemistry, Paul Scherrer Institute, 5232 Villigen, Switzerland*
[o] *Atmospheric Pollution Laboratory (LCA), Department of Applied Physics, Miguel Hernández University, Avenida de la Universidad S/N, 03202, Elche, Spain*
[p] *Arpa Lombardia, Settore Monitoraggi Ambientali, Unità Operativa Qualità dell'Aria, Milano, Italy*
[q] *Institute of Atmospheric Sciences and Climate-National Research Council, Rome, Italy*
[r] *MRC Centre for Environment and Health, Environmental Research Group, Imperial College London, UK*
[s] *HPRU in Environmental Exposures and Health, Imperial College London, UK*
[t] *Laboratory for Air Pollution and Environmental Technology, Swiss Federal Laboratories for Materials Science and Technology (Empa), Duebendorf, Switzerland*
[u] *Institute for Environmental Research & Sustainable Development, National Observatory of Athens, Athens, Greece*
[v] *Atmospheric Composition Research, Finnish Meteorological Institute, Helsinki, Finland*
[w] *ARPA Lazio, Regional Environmental Protection Agency, Rome, Italy*
[x] *Center for Atmospheric Research, University of Nova Gorica, Nova Gorica, 5270, Slovenia*
[y] *Jozef Stefan Institute, Ljubljana, 1000, Slovenia*
[z] *Helsinki Region Environmental Services Authority (HSY), Helsinki, Finland*
[aa] *Laboratory of Aerosols Chemistry and Physics, Institute of Chemical Process Fundamentals, Academy of Sciences of the Czech Republic, Rozvojova, Prague, Czech Republic*
[ab] *Laboratoire des Sciences du Climat et de l'Environnement, CEA/Orme des Merisiers, Gif-sur-Yvette, France*
[ac] *Division of Air Resources, New York State Dept of Environmental Conservation, NY, USA*
[ad] *Division of Environmental Health & Risk Management, School of Geography, Earth & Environmental Sciences, University of Birmingham, Edgbaston, Birmingham, United Kingdom*
[ae] *Department of Environmental Sciences, Faculty of Meteorology, Environment and Arid Land Agriculture, King Abdulaziz University, Jeddah, Saudi Arabia*
[af] *Institute for Atmospheric and Earth System Research/Physics (INAR), Faculty of Science, University of Helsinki, Helsinki, Finland*

* Corresponding authors at: Institute of Environmental Assessment and Water Research (IDAEA-CSIC), Barcelona, Spain.
E-mail addresses: marjan.savadkoohi@idaea.csic.es (M. Savadkoohi), marco.pandolfi@idaea.csic.es (M. Pandolfi).

https://doi.org/10.1016/j.envint.2024.108553
Received 20 December 2023; Received in revised form 1 March 2024; Accepted 1 March 2024
Available online 2 March 2024

ARTICLE INFO

Handling Editor: Olga Kalantzi

Keywords:
eBC
MAC
FAPs
EC
Absorption
Site specific MAC
Rolling MAC

ABSTRACT

A reliable determination of equivalent black carbon (eBC) mass concentrations derived from filter absorption photometers (FAPs) measurements depends on the appropriate quantification of the mass absorption cross-section (MAC) for converting the absorption coefficient (b_{abs}) to eBC. This study investigates the spatial–temporal variability of the MAC obtained from simultaneous elemental carbon (EC) and b_{abs} measurements performed at 22 sites. We compared different methodologies for retrieving eBC integrating different options for calculating MAC including: locally derived, median value calculated from 22 sites, and site-specific rolling MAC. The eBC concentrations that underwent correction using these methods were identified as *LeBC* (*local* MAC), *MeBC* (*median* MAC), and *ReBC* (*Rolling* MAC) respectively. Pronounced differences (up to more than 50 %) were observed between eBC as directly provided by FAPs (*NeBC*; Nominal instrumental MAC) and ReBC due to the differences observed between the experimental and nominal MAC values. The median MAC was 7.8 ± 3.4 $m^2\ g^{-1}$ from 12 aethalometers at 880 nm, and 10.6 ± 4.7 $m^2\ g^{-1}$ from 10 MAAPs at 637 nm. The experimental MAC showed significant site and seasonal dependencies, with heterogeneous patterns between summer and winter in different regions. In addition, long-term trend analysis revealed statistically significant (s.s.) decreasing trends in EC. Interestingly, we showed that the corresponding corrected eBC trends are not independent of the way eBC is calculated due to the variability of MAC. NeBC and EC decreasing trends were consistent at sites with no significant trend in experimental MAC. Conversely, where MAC showed s.s. trend, the NeBC and EC trends were not consistent while ReBC concentration followed the same pattern as EC. These results underscore the importance of accounting for MAC variations when deriving eBC measurements from FAPs and emphasize the necessity of incorporating EC observations to constrain the uncertainty associated with eBC.

1. Introduction

Black Carbon (BC) is one of the key targets for current research on air quality (AQ). The definition of BC is highly reliant on the measurement techniques employed, and one of the main challenges in this regard is the lack of a systematic approach to harmonize BC concentrations obtained from various measurement instruments, thus causing difficulties when comparing data across different monitoring sites (Ciupek et al., 2021). To address this concern, efforts to establish more standardized methodologies for reporting atmospheric BC are required. Commonly, BC mass concentrations are determined indirectly by optical instruments (e.g., Bond et al., 2013). Filter absorption photometers (FAPs) such as aethalometer (AE) and multi-angle absorption photometers (MAAP) provide continuous BC data by measuring light attenuation from particles collected on a filter at specific wavelengths. The measured attenuation is converted to absorption coefficient (b_{abs}) and then into equivalent black carbon (eBC) mass concentrations using pre-defined mass absorption cross-sections (MAC). In this case, according to Petzold et al. (2013), the term eBC should be used instead of BC as a proxy of b_{abs} when FAPs are employed.

To estimate eBC mass concentrations, harmonized measurements of b_{abs} from FAPs and reliable determination of MAC values are essential. The prevalent approach for converting the b_{abs} to eBC mass concentration involves applying the instrument manufacturers fixed MAC values that were obtained through optical methods (Bond and Bergstrom, 2006; Snyder and Schauer, 2007). MAAP uses the constant MAC value of 6.6 $m^2\ g^{-1}$ at a nominal wavelength of 637 nm to convert the optically measured b_{abs} to eBC mass concentration. The MAC value for the MAAP at $\lambda = 637$ nm were derived through the comparison of b_{abs} (MAAP) and BC mass concentrations (M_{BC}) measurements conducted at four sites in Germany (Petzold and Schönlinner, 2004) using the German reference method VDI2465 Part 1 (GRM, Schmid et al., 2001). The multi-wavelength dual-spot AE, (AE33, Magee Scientific) applies a nominal MAC value of 7.77 $m^2\ g^{-1}$ at 880 nm which is the reference wavelength for providing eBC from AE instruments. The value of 7.77 $m^2\ g^{-1}$ at $\lambda =$ 880 nm was initially determined through the comparative analysis of optical and thermal measurements on filters loaded with refractory carbonaceous material (Gundel et al., 1984) and traced to new optical measurements (Drinovec et al., 2015). Older AE models, 7-wavelengths AE31 and 2-wavelengths AE21 and AE22 (operating at 370 and 880 nm), employ a mass attenuation cross-section of 16.62 $m^2\ g^{-1}$ at 880 nm (Gundel et al., 1984). The ratio between the mass attenuation and absorption cross sections is the multiple-scattering enhancement factor (C_0) of 2.14 that accounts for artifacts associated with the presence of the filter tape (Weingartner et al., 2003).

While nominal MAC values are used by FAPs for converting b_{abs} to eBC mass concentration, empirical studies revealed a wide range of experimental MAC values across different sites. Indeed, MAC is considerably variable and it is influenced by factors such as location e.g., urban, rural, and high-altitude (Salako et al., 2012; Wang et al., 2013) BC particle size (Zhao et al., 2021), internal mixing (Cao et al., 2015; Cho et al., 2019; Knox et al., 2009; Yuan et al., 2021; Zanatta et al., 2016), combustion sources (Olson et al., 2015; Wu et al., 2021), selected b_{abs} wavelengths (Mbengue et al., 2021; Srivastava et al., 2022), monitoring periods (Ciupek et al., 2021; Ram and Sarin, 2009), and instrument types (Kondo et al., 2009; Nordmann et al., 2013). For instance, freshly emitted uncoated eBC has been reported to have a MAC of approximately 7.5 ± 1.2 $m^2\ g^{-1}$ at 550 nm (Bond and Bergstrom, 2006), confirmed by a recent study where an average MAC of about 8.0 ± 0.7 $m^2\ g^{-1}$ at 550 nm was reported (Liu et al., 2020). However, atmospheric eBC particles can have a wide range of MAC values. For example, Presler-Jur et al. (2017) reported values ranging from 6.9 to 9.4 $m^2\ g^{-1}$ in different U.S. regions and seasons. Similarly, Nordmann et al. (2013) found MAC values ranging from 3.9 to 7.4 $m^2\ g^{-1}$ at 550 nm across Central Europe, while Mbengue et al. (2021) reported a range of 7.84 ± 2.79 $m^2\ g^{-1}$ at 660 nm to 13.90 ± 4.97 $m^2\ g^{-1}$ at 370 nm. Wu et al. (2021) observed MAC values ranging from 2.71 to 5.91 $m^2\ g^{-1}$ at 870 nm for different combustion sources, including biofuel stoves and diesel trucks. Ciupek et al. (2021) reported varied MAC values at different London sites, ranging from 7.4 to 12.6 $m^2\ g^{-1}$ at 880 nm. Additionally, studies by Srivastava et al. (2022), Grange et al. (2020), Pandolfi et al. (2014), and Zanatta et al. (2016) have provided further insights into the range of MAC values across different measurement sites and regions.

The variation of these experimental MAC values causes difficulties in determining accurate eBC mass concentration and, consequently, in properly representing eBC in AQ models (Grange et al., 2020; Ciupek et al., 2021). These problems arise because using the nominal MAC from FAPs without considering the observed MAC spatial–temporal variability can result in misleading eBC estimations (e.g., Ciupek et al., 2021; Moschos et al., 2021; Srivastava et al., 2022). When employing a nominal MAC, although the b_{abs} data might be comparable, the resulting eBC concentrations may not be directly comparable across different sites. For this reason, the determination of in situ MAC holds significant importance for constraining uncertainty in eBC derived from FAPs measurements (Kondo et al., 2009; Zhao et al., 2021). As shown here and reported elsewhere (e.g., Ciupek et al., 2021; Mbengue et al., 2021;

Pileci et al., 2021), having simultaneous FAPs and EC measurements helps providing more reliable and accurate estimation of high time resolution eBC from FAPs (Grange et al., 2020; Helin et al., 2018; Ivančič et al., 2022; Srivastava et al., 2022).

Furthermore, the incorporation of eBC in the new European Union (EU) directive (Council of the European Union, 2023) evidences a growing awareness of the need to address the eBC adverse effects on both human health and the environment (Janssen et al., 2011, Janssen et al., 2012; Karamfilova, 2022; Kuula et al., 2022). In fact, the current revision of the EU ambient AQ directive and World Health Organization AQ Guideline (WHO-AQG) also emphasize the importance of monitoring eBC concentrations to gain new insights into its impact on AQ and climate (WHO, 2021). To incorporate eBC as a new variable in AQ guidelines and to develop effective mitigation strategies, it is crucial to estimate its mass concentration in a consistent way throughout the air quality monitoring networks (AQMNs) with minimal uncertainties. In response to these growing demands for standardized and reliable estimation of eBC, various initiatives have been undertaken by research infrastructures such as ACTRIS, EURAMET (STANBC, 2023) and the Working Group WG35 of the European Committee for Standardization (CEN). These entities have highlighted the significance of harmonizing eBC measurement procedures to ensure consistency and comparability of data across different monitoring networks and within research studies. Through their efforts, comprehensive recommendations and guidelines are being developed to establish robust protocols, including various sampling techniques, instruments, and data processing methodologies (ACTRIS-ECAC, 2022). Here we present a robust, sensitivity analysis of MAC values and eBC mass concentration to support these guidelines.

2. Methodology

In this study, we quantified the mass concentrations of eBC through in situ MAC assessment at 22 sites to: i) normalize eBC observations across the sites and ii) propose more advanced methods to determine site-specific eBC mass concentrations. These objectives align with the aim of measurement consistency and minimizing instrument-to-instrument variability observed in the intercomparison of FAPs (Asmi et al., 2021; Cuesta-Mosquera et al., 2021; Helin et al., 2018; Müller et al., 2011; Pileci et al., 2021). Furthermore, our approach uses different levels of correction schemes for eBC estimation including the determination of median MAC value for the 22 sites and site-specific and rolling regression MAC values. The rolling approach has been recently suggested by Grange et al. (2020) and consists of continuous EC measurements over an extended period. It was proposed to be an efficient way to refine eBC mass concentrations. Within this context, the primary focus of this study was to perform a comparative analysis between various methods to estimate eBC mass concentrations. Following this, site-specific MAC values can be determined for each of the 22 sites where EC concentration data were available. Additionally, this study explored potential long-term variations in experimental MAC across the sites.

2.1. Measurement sites

Out of the 50 European monitoring sites supplying FAPs data to the RI-URBANS project (Savadkoohi et al., 2023), 22 sites (21 EU, 1 US) also provided EC mass concentration measurements. Table 1 presents an overview of the sites and instruments used for in situ measurements of eBC and b_{abs} from FAPs and EC mass concentrations. The 22 measurement sites from 18 cities used here include urban background (UB, 13 sites), traffic (TR, 4 sites), sub-urban (SUB, 2 sites) and regional background (RB, 3 sites) sites (Fig. 1).

2.2. Instrumentation

In this study, the employed FAPs were the AE33 (9 out of 22 sites) and the MAAP (10 out of 22 sites). Additionally, three sites (LND_UB, LND_TR, and ROC_UB) provided data using the AE22 or AE21 models. The EC mass concentrations were measured using thermal-optical organic/elemental carbon, OC-EC Sunset analyzers either offline or online (Karanasiou et al., 2020). MAAP instruments account for compensation of filter-loading-induced artifacts, that impact the b_{abs} calculation (Petzold and Schönlinner, 2004), simultaneously measuring the intensity of light transmitted through the aerosol-loaded filter tape and scattered back from the filter spot, and subsequently converts these data to particle light absorption. The MAAP specifies a measurement wavelength of 670 nm, although its actual wavelength is 637 nm (Müller et al., 2011). The default setting for the MAC is 6.6 m^2/g, enabling the conversion of optically measured b_{abs} data into eBC mass concentrations. The AE33 dual-spot Aethalometer (Magee Scientific) measures light attenuation (σ_{ATN}) through aerosol-loaded filter tape and determines b_{abs} at seven distinct wavelengths (370, 470, 520, 590, 660, 880, and 950 nm) using an assumed wavelength-dependent MAC and a wavelength independent filter multiple-scattering parameter (C_0). The AE33 converts the optical absorption coefficients into eBC mass concentrations using a nominal MAC value of 7.77 m^2/g at 880 nm and default C_0 values that depend on the filter tape used (e.g. Savadkoohi et al., 2023). Filter loading effects are measured and corrected online using algorithms implemented in AE33 (Drinovec et al., 2015). Older AE models such as the AE22, and AE21 were used at three sites (i.e., LND_UB, LND_TR, and ROC_UB) to measure σ_{ATN} through the filter at two (AE22, and AE21; 370 and 880 nm) wavelengths using an instrument-derived mass attenuation cross section value of 16.62 m^2/g at 880 nm. However, these models required a manual post-processing correction for loading effects, and algorithms for correcting this artifact have been developed and tested by different researchers (Collaud Coen et al., 2010; Virkkula et al., 2007; Weingartner et al., 2003). More detailed information on these techniques can be found in previous reports (e.g., Drinovec et al., 2015; Müller et al., 2011; Petzold et al., 2005; Petzold and Schönlinner, 2004; Savadkoohi et al., 2023).

2.3. Data processing

Over the long-time span of the compiled datasets, the minimum data coverage was one year to the maximum twelve years. Fig. S1 visualizes the distribution of eBC dataset, including data coverage, data capture, and missing data from FAPs at 22 sites. Regarding FAPs measurements, Level 2 quality assured/quality checked (QA/QC) data from the EBAS database (EBAS, https://ebas.nilu.no/) were used for three sites (LEJ_TR1, GRA_UB and IPR_RB). For the other sites, data providers directly supplied hourly averaged data as either NeBC mass concentrations, or b_{abs}. To ensure the comparability of measurements across the sites, data were processed using harmonized measurement protocols according to the ACTRIS recommendations for reporting b_{abs} from FAPs (Müller and Fiebig, 2018a, 2018b). More details of the methodology employed to derive b_{abs} and subsequently estimate eBC mass concentrations are available in detail in Fig. 2 of Savadkoohi et al. (2023). For most monitoring sites, NeBC concentrations were directly supplied by data providers and used for defining the b_{abs}. In cases where b_{abs} data were provided (BER_TR, ZUR_UB, PAY_RB, ATH_SUB), eBC mass concentrations were determined by employing nominal MAC values and harmonization factors (H*). This harmonization process involves the application of instrument-specific H* factor to convert the light attenuation captured by FAPs into b_{abs}. ACTRIS H* factors have been established to ensure consistency and comparability of b_{abs} data for different instruments and measurement sites (Müller and Fiebig, 2018a; Laj et al., 2020; Müller et al., 2011; Zanatta et al., 2016). Further details regarding the appropriate selection of the C_0 and the standardized H* factors can be found in Savadkoohi et al. (2023). As previously mentioned, AE33

Table 1
Characteristics and instrumental details of the 22 measurement sites supplying eBC and EC mass concentrations data. Table contains detailed information such as the location of each site, the type of the site (UB, Urban Background; TR, Traffic; SUB, Suburban Background; RB, Regional Background), the FAPs used for measurements, and specific measurement details. Finland (FI), United Kingdom (UK), United States (US), France (FR), Spain (ES), Greece (GR), Germany (DE), Switzerland (CH), Italy (IT), Czech Republic (CZ).

Site	City-Country	Station Type	Acronym	Coordinates	Data provider	Cut-off eBC	FAPs	Wavelengths (λ)	Nominal MAC (m^2/g)	EC measurement method: Online/offline	Thermal-optical protocol	Cut-off EC
Palau Reial	Barcelona-ES	UB	BCN_UB	41.387, 2.115	IDAEA-CSIC	PM10	MAAP	637 nm	6.6	Offline	EUSAAR-2	PM_{10}
UGR	Granada-ES	UB	GRA_UB	37.18, −3.58	Universidad de Granada	Total	MAAP	637 nm	6.6	Offline	EUSAAR-2	PM_{10}
Longchamp	Marseille-FR	UB	MAR_UB	43.305, 5.394	AtmoSud-LCE	PM2.5	AE33	880 nm	7.77	Offline	EUSAAR-2	PM_1
Dresden-Winckelmannstrasse	Dresden-DE	UB	DDW_UB	51.036, 13.730	LfULG	PM1	MAAP	637 nm	6.6	Offline	EUSAAR-2	PM_1
North Kensington	London-UK	UB	LND_UB	51.521, −0.213	Imperial College	PM2.5	AE22	880 nm	7.77	Offline	QUARTZ until 01/Feb/2016, EUSAAR2 from 03/Feb/2016	PM_{10} until 27/Feb/2019, $PM_{2.5}$ from 01/Mar/2019
Rochester	Rochester-US	UB	ROC_UB	43.146, −77.542	NYS Dept of Environment	PM2.5	AE21	880 nm	7.77	Offline	IMPROVE-A	$PM_{2.5}$
Bollwerk	Bern-CH	TR	BER_TR	46.951, 7.441	EMPA	PM2.5	AE31-AE3	880 nm	7.77	Offline	EUSAAR-2	$PM_{2.5}$
Kaserne	Zurich-CH	UB	ZUR_UB	47.378, 8.530	EMPA	PM2.5	AE31-AE33	880 nm	7.77	Offline	EUSAAR-2	$PM_{2.5}$
NOA	Athens-GR	UB	ATH_UB	37.973, 23.718	NOA	PM10-PM2.5	AE33	880 nm	7.77	Offline	EUSAAR-2	$PM_{2.5}$
Villa Ada	Rome-IT	UB	ROM_UB	41.932, 12.507	CNR-ISAC	PM1	AE33	880 nm	7.77	Offline	EUSAAR-2	$PM_{2.5}$
Pascal	Milan-IT	UB	MLN_UB	45.464, 9.188	Arpa Lombardia	PM10	MAAP	880 nm	7.77	Offline	EUSAAR-2	PM_{10}
Dresden-Nord	Dresden-DE	TR	DRD_TR	51.064, 13.7413	LfULG	PM1	MAAP	637 nm	6.6	Offline	EUSAAR-2	PM_{10}
Mäkelänkatu	Helsinki-FI	TR	HEL_TR2	60.196, 24.952	HSY	PM1	MAAP	637 nm	6.6	Offline	EUSAAR-2	PM_1
Mitte	Leipzig-DE	TR	LEJ_TR1	51.344, 12.377	TROPOS	PM10	MAAP	637 nm	6.6	Offline	EUSAAR-2	PM_{10}
Marylebone Road	London-UK	TR	LND_TR	51.522, −0.1546	Imperial College	PM2.5	AE22	880 nm	7.77	Offline	QUARTZ until 01/Feb/2016, EUSAAR2 from 03/Feb/2016	PM_{10} until 08/Oct/2019, $PM_{2.5}$ from 10/Oct/2019
Demokritos	Athens-GR	SUB	ATH_SUB	37.99, 23.82	NCSR	PM10	AE33	880 nm	7.77	Online	EUSAAR-2	$PM_{2.5}$
Sirta	Paris-FR	SUB	PAR_SUB	48.7086, 2.1588	LSCE/INERIS	PM1	AE33	880 nm	7.77	Offline	EUSAAR-2	$PM_{2.5}$
Ispra	Ispra_IT	RB	IPR_RB	45.8, 8.633	EC-JRC-IES	PM10	MAAP	637 nm	6.6	Online	EUSAAR-2	$PM_{2.5}$
SMEAR II	Hyytiälä-FI	RB	SMR_RB	61.847, 24.295	University of Helsinki	PM10	MAAP	637 nm	6.6	Online	EUSAAR-2	$PM_{2.5}$
Payerne	Payerne-CH	RB	PAY_RB	46.813, 6.944	EMPA	PM10	AE31-AE33	880 nm	7.77	Offline	EUSAAR-2	$PM_{2.5}$
Prague Suchdol	Prague-CZ	UB	PRG_UB	50.1268, 14.384	ICPF	PM10	MAAP	637 nm	6.6	Online	EUSAAR-2	PM_1
UMH	Elche-ES	UB	UMH_UB	38.2785, 0.6878	Universitat Miguel Hernández de Elche	PM10	AE33	880 nm	7.77	Offline	EUSAAR-2	PM_{10}

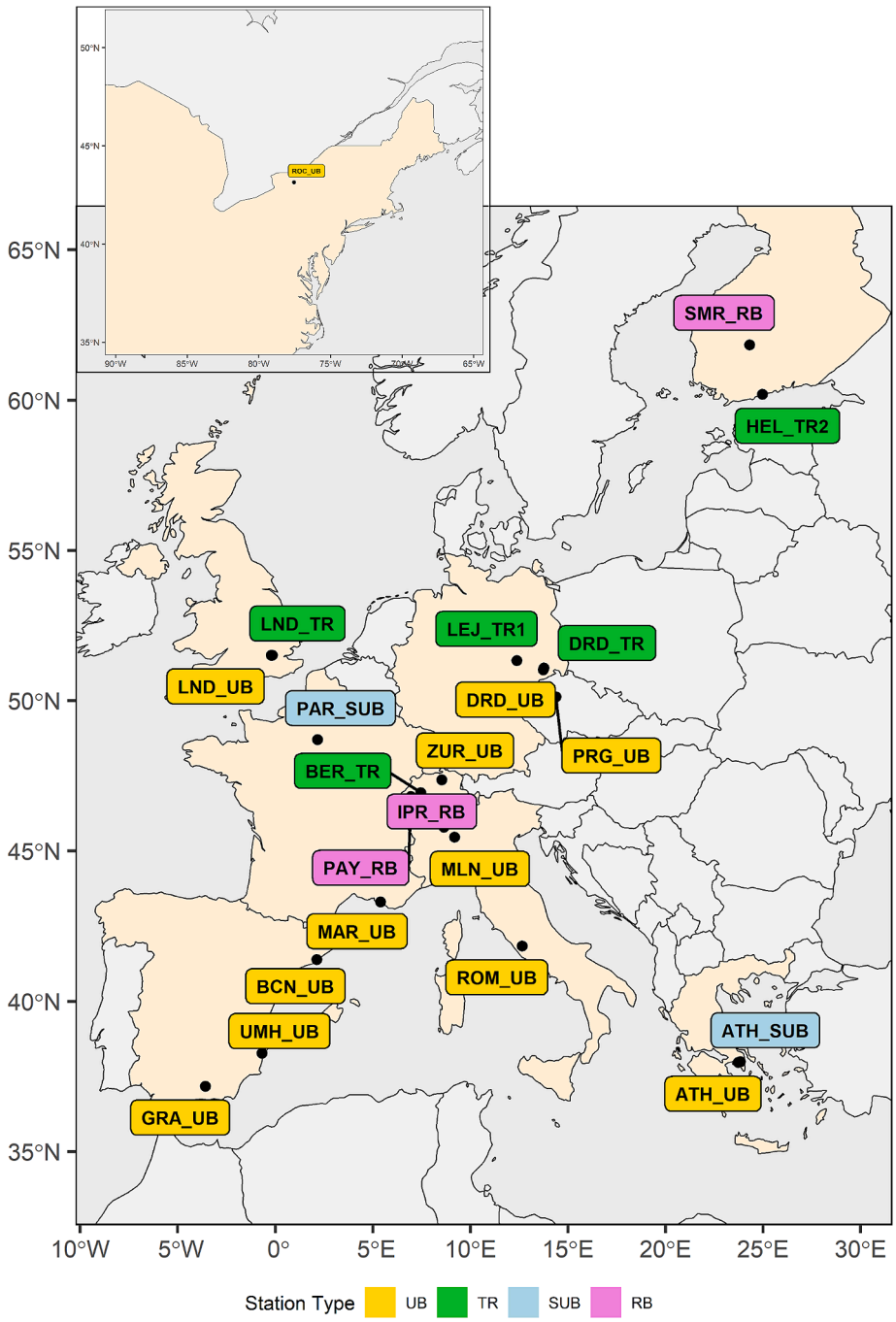

Fig. 1. Location of the cities and type of 22 monitoring sites with eBC and EC mass concentration measurement data being supplied to this study, UB, urban background; SUB, suburban background; TR, traffic; RB, regional background.

instruments were already equipped with online factor loading corrections (Drinovec et al., 2015), while data obtained from older AE models (AE21 and AE22) were corrected offline by the data providers. Specifically, the correction scheme proposed by Turner et al. (2007) was applied to the AE21 data from ROC_UB (Rattigan et al., 2013), whereas the scheme introduced by Virkkula et al. (2007) was applied to the AE22 data from LND_UB/LND_TR. The AE31 data from ZUR_UB, BER_TR and PAY_RB has been compensated for the filter-loading using schemes introduced by Drinovec et al. (2015) and Weingartner et al. (2003).

2.4. Mass absorption cross-section (MAC) of equivalent black carbon

The procedure used to obtain in situ MAC from the collocated measurements of EC and b_{abs} at each site is summarized in Fig. 2. MAC values obtained using this method are hereafter referred to as experimental or site-specific MAC. To construct the necessary dataset for analysis, the AE and MAAP measurements were aggregated to match the EC time resolutions. Unlike the continuous measurements of eBC obtained from FAPs, the EC observations were available with varying sampling intervals spanning from 1 to 12 days and different time resolutions typically ranging from 1, 3 to 12, or 24 h. Considering this, the dates corresponding to both EC and eBC observations were matched, resulting in creation of a self-consistent database (see step 1, Fig. 2). No efforts were made to impute or interpolate missing observations, and incomplete data were excluded from the datasets to mitigate potential errors. Data processing and statistical analysis were performed using R

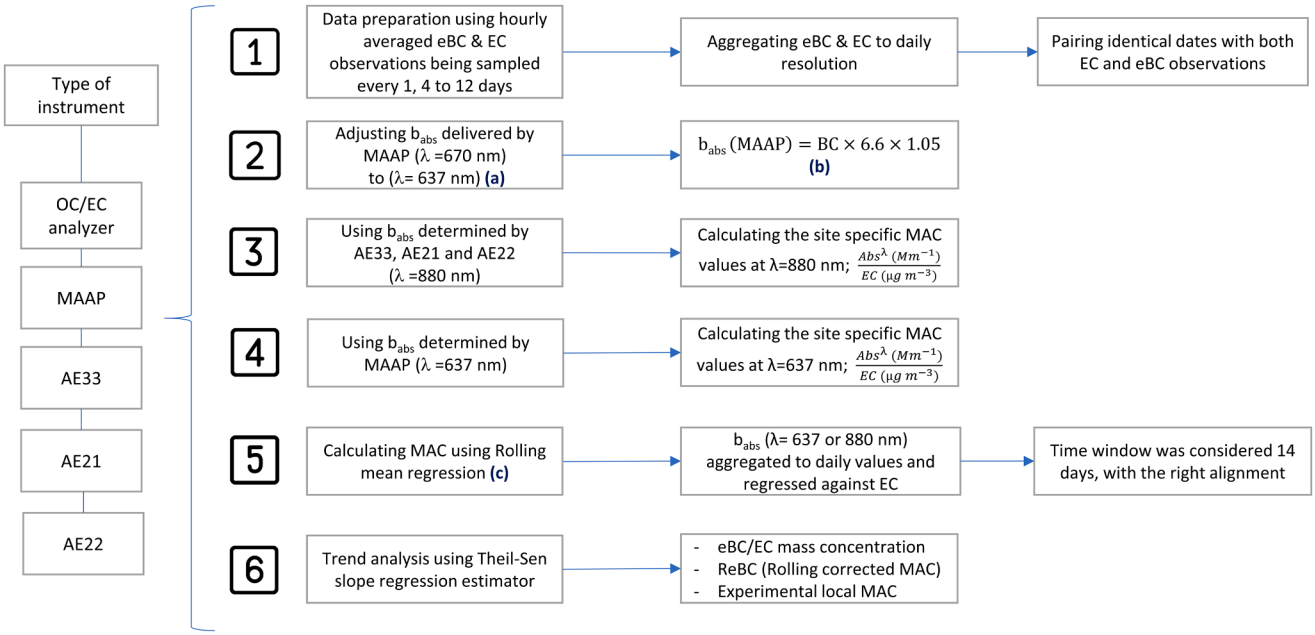

Fig. 2. The overall scheme by which to process corrected and normalized eBC mass concentrations in order to obtain site-specific MAC values. More details are provided in Sections 2.4. (a): 637 nm is the reference wavelength of the MAAP to derive MAAP- equivalent absorption coefficient; (b): 1.05 is the correction factor to the true wavelength (637 nm); (c) Efficient Rolling/Windowed Operations using "zoo" and "RcppRoll" R packages.

statistical computing software. Specifically, the following packages were used: openair (Carslaw and Ropkins, 2012), zoo: S3 infrastructure for regular and irregular time series (Zeileis and Grothendieck, 2005), the 'RcppRoll' package (Ushey, 2022) and other R data analysis packages that enabled efficient rolling computations.

Given that eBC and EC particles are mostly submicron, variations in the cut-off inlets for their measurements would introduce minimal uncertainty and the overall accuracy of eBC and EC measurements should remain relatively unaffected. Moreover, the reported uncertainty for the b_{abs} of MAAP at 637 nm is 15 %, as stated by Zanatta et al. (2016) and Müller et al. (2011), while Petzold and Schönlinner (2004) have reported uncertainties of 12 % for b_{abs} at 637 nm. Additionally, Valentini et al. (2021) and Yus-Díez et al. (2021) and references herein, reported a possible overestimation of the b_{abs} from MAAP compared to other non-reference techniques for measuring absorption. Regarding the AE33, uncertainties of around 15 % and 25 % have been reported for b_{abs} and eBC, respectively (Rigler et al., 2020). The uncertainty of the estimated MAC for MAAP, according to Zanatta et al. (2016), is around 29 % when EC is measured with EUSAAR-2 Protocol. In our study, the uncertainty associated with the MAC at 880 nm is estimated to be around 30–35 % considering the use of filter types M8020 and M8060 and the reference C values as discussed by Yus-Díez et al. (2021). Despite the additional uncertainty in the absorption measurements provided by AE33 due to variations of the C factor, we use the term MAC in this work irrespective of the FAP used for its calculation to be consistent with the terminology widely used in literature for reporting mass absorption cross section. Taking this into account, the additional aforementioned uncertainties in the measurements of b_{abs} can be minimized by continuously correcting the calculated eBC with simultaneous EC measurements following the CEN standards (European Committee for Standardisation, 2017).

Moreover, the uncertainties associated with EC measurements, arising from both offline and online methods, cannot be disregarded in the determination of experimental MAC. As previously estimated, the deviation in EC average concentrations between Semi-Continuous and offline analyzers was quantified at 18 %, following the procedures outlined in the EN 16909:2017 standard (Karanasiou et al., 2020). Furthermore, a laboratory-to-laboratory variability of 10 % in EC data has been reported by Rigler et al. (2020). This is associated with uncertainties related to the OC-EC split point, influenced by aerosol type and chemical composition and charring of organic material in thermal optical methods (Karanasiou et al., 2020; Rigler et al., 2020). Earlier studies have indicated a range of uncertainties in EC determination, spanning from 2 to 7 %, in accordance with the EUSAAR-2 protocol in Europe (Cavalli and Putaud, 2010; Karanasiou et al., 2015).

To obtain the experimental MAC values at each site, the b_{abs} wavelengths from the MAAP (637 nm), AE33, AE21, and AE22 instruments (880 nm), were used. The calculations were performed using the equations outlined in steps 3 and 4 of Fig. 2. The determination of experimental MAC was obtained as the ratio of the b_{abs} to EC mass concentration "$MAC^{\lambda} = \frac{Abs^{\lambda}}{[EC]}$". This calculation was performed using the averaged b_{abs} over a 24-hour period (Grange et al., 2020; Laborde et al., 2013; Pileci et al., 2021). An alternative approach to account for temporal variations in MAC is the implementation of a rolling simple least-squares linear regression model, which relates daily aggregated b_{abs} values to corresponding EC concentrations, resulting in rolling mean MAC values. Grange et al. (2020) previously applied this method and demonstrated its potential for achieving consistent results. Applying this approach to the compiled datasets allowed for comparisons between NeBC and ReBC mass concentrations obtained through the rolling method (see step 5; Fig. 2). For the rolling mean regression technique (Zeileis and Grothendieck, 2005), a 14-day right-aligned time window was selected appropriate, differing from a 180-day center-aligned window used by Grange et al. (2020). The choice of window size depended on the data's sample size and periodicity, with shorter windows suitable for shorter intervals and larger windows for longer ones. More detail on the rolling method is provided in the supplementary information, where a sensitivity study is performed (Fig. S2).

The numbers of observations used to calculate the site-specific MAC were not consistent across the sites. For example, the EC filter samples collected at the HEL_TR2 site consisted of only 38 daily observations, which may not be representative of the area (Helin et al., 2018). Conversely, the sites PAR_SUB and IPR_RB had the highest number of compiled EC observations which can provide more robust statistical confidence. To study the statistical significance of variations in the mean of the experimental MAC in different seasons, we initially performed a normality test to examine the homogeneity of variances among various

sites and seasons. This step aimed to determine the appropriateness of selecting either the parametric analysis of variance (ANOVA) or the non-parametric Kruskal-Wallis test, followed by the Dunn's test. The selection of an appropriate statistical approach was contingent upon the fulfillment of assumptions regarding the data distribution and homogeneity of variances.

2.5. Trend analysis

The method employed for the trend analysis (step 6; Fig. 2) was a Theil-Sen slope regression estimator, a robust, non-parametric estimator provided by the openair R package (Carslaw and Ropkins, 2012). The aim of this analysis was to assess the statistical significance and slopes of long-term trends in NeBC, ReBC and EC mass concentrations, as well as the experimental MAC at 637 or 880 nm. Theil-Sen method accurately calculates 95 % confidence intervals, even when dealing with non-normal data and non-constant error variance, and it is also resilient to outliers. Only monitoring sites that had at least 9 years of continuous eBC and EC mass concentration data, with a minimum of 75 % valid measurements during that period, were considered for the trend analysis (i.e., BCN_UB, ROC_UB, IPR_RB, PAR_SUB, and ZUR_UB).

3. Results and discussion

3.1. Spatial variability of experimental mass absorption cross-section (MAC)

Fig. 3 shows box plots of the experimentally determined MAC for MAAPs and AEs, normalized through concurrent EC measurements by site typology. The internal black solid line within the boxplots indicates the median value, distinguished by instrument type and measuring wavelengths (637 nm and 880 nm). The distribution and spread of these box plots provide the range of EC-derived MAC values and their variability. The MAC variability over the sampled sites was not geographically dependent and no consistent pattern was observed in the deviation of the experimental MAC values. The median experimental MAC value of 10.6 ± 4.7 m^2 g^{-1} (range: 7–14 m^2 g^{-1}; Fig. 3) was obtained for MAAP measurements at 637 nm across 10 sites. This experimental median MAC value is close to the value of 10.0 m^2 g^{-1} previously proposed by Zanatta et al. (2016) for MAC, using data from European RB sites measured from FAPs at 637 nm. The median MAC value of 7.8 ± 3.4 m^2 g^{-1} (range: 5–12 m^2 g^{-1}; Fig. 3) was determined at 880 nm for AE measurements at 12 sites (see Fig. 3). The relative percent deviation from the median, obtained as 16 % for MAAP, whereas AEs deviated by 37 %. Despite the large variability of the reported MAC, it is important to note that the median AE33 MAC reported here (7.8 m^2 g^{-1}) is very close to the nominal AE33 MAC of 7.77 m^2 g^{-1} at 880 nm. However, despite this similarity, the nominal eBC reported by the AE33 is overestimated by around 50 % due to the filter multiple-scattering parameter (C_0) as the main source of uncertainty (e.g., Savadkoohi et al., 2023). In the case of the MAAP, the eBC reported by the MAAP is mostly affected by the nominal MAC used (6.6 m^2 g^{-1}) which is much lower compared to the MAC value of 10.6 m^2 g^{-1} reported here.

3.2. Site-specific mass absorption cross-section (MAC)

Table 2 contains the site-specific MAC values presented in Fig. 3. According to the data presented in Table 2, among the urban sites, the highest site-specific MAC values were observed at PRG_UB, MLN_UB, DDW_UB, and GRA_UB. To consider the potential contributors, MLN_UB, has been previously recognized to be influenced by the emissions from biomass burning (BB) specifically during winter (Mousavi et al., 2019). DDW_UB is located 1.7 km away from the city center, is grouped into the strongly traffic influenced site and is usually influenced by the plumes of BC originating from domestic heating in Eastern Europe (Sun et al., 2020, 2019). In GRA_UB, there is also a large influence of open BB for agricultural waste removal at the agricultural lands surrounding the city (Casquero-Vera et al., 2021; Titos et al., 2017). This additional source together with low wind dispersion and frequent temperature inversions during the cold season facilitates the accumulation of aged secondary aerosols (van Drooge et al., 2022) at this site. In PRG_UB, the sampling site is located in a residential area prone to domestic heating at the north-west suburb of the city, about 250 m from the nearest road, and 8 km from the international Václav Havel airport (Zíková et al., 2016). Different origins of carbonaceous aerosols have also been observed at this site mainly from combustion (biomass, coal for heating) in winter and biogenic aerosols in summer (Vodička et al., 2023, 2022).

Among traffic sites, higher site-specific MAC values were observed at the HEL_TR2 and LEJ_TR1 sites. LEJ_TR1 is in a central city area along a roadside. This site was primarily characterized by elevated particle number concentrations (PNCs), which can be attributed to the freshly emitted and quickly nucleated particles from traffic exhaust emissions (Sun et al., 2020; Trechera et al., 2023). HEL_TR2 is located on the curbside of a busy traffic street referred to as street canyon (SC, Mäkelänkatu) in Northern Europe. Air quality at this site has been reported to be influenced by high traffic density (Barreira et al., 2021; Helin et al., 2018). Between the two SUB sites, ATH_SUB showed an elevated MAC in contrast to PAR_SUB that can be attributed to both traffic-related and BB sources (Diapouli et al., 2017). This station is exposed to transported pollutants originating from the urban area of Athens under most atmospheric conditions (Gini et al., 2022). Among the RB sites, the observed high MAC value at IPR_RB, can be attributed to local emissions, local meteorology, long-ranged transport, and its topography (Pandolfi et al., 2018; Putaud et al., 2014). PAY_RB showed a high MAC value. In previous studies, a significant increase in MAC values at PAY_RB was observed, possibly due to instrument artifacts. This increase coincided with instrument replacement in June 2016, after which MAC values showed reduced variability (Grange et al., 2020). Alternatively, sites like ZUR_UB, BER_TR, MAR_UB, and PAR_SUB exhibited low MAC values, indicative of potential influence from diverse sources of eBC, and other specific characteristics of the sampling site, such as local emissions, meteorological conditions, and geographical features.

Fig. 4 presents the frequency distribution of the experimental MAC values at 637 and 880 nm based on instrument type across 22 sites throughout the entire measurement period with a skewness bias at ZUR_UB, BER_TR, MAR_UB, and PAR_SUB. Notably, both MLN_UB and IPR_RB showed a greater degree of dispersion in the distribution pattern. The underlying factors that contribute to the bimodality in some sites as PAY_RB, BER_TR and ROM_UB may indicate the presence of distinct sources contributing to the observed MAC values representing different physical or chemical processes affecting b_{abs}. This might be linked to seasonal or temporal variations or arise from instrument-related factors or measurement artifacts. The variation in the standard deviations of MAC values, indicates changes in average aerosol characteristics on a regular basis, which are generally influenced by varying sources that may differ between summer and winter seasons.

Understanding the temporal and spatial variability in MAC requires considering studies using similar measurement techniques, e.g., MAAP and AEs, at consistent wavelengths. Direct comparisons might be difficult due to site differences, seasonal variations, and measurement methodologies. Experimental MAC values in the literature were mainly reported from short-term campaigns, limiting direct site-to-site comparisons. In addition, seasonal changes affect eBC emissions and therefore, MAC, emphasizing the need for long-term measurements to derive site-specific MAC values. These variations relate to aerosol composition, instrument responses, and time-dependent factors (Ram and Sarin, 2009; Yuan et al., 2021). Heterogeneous carbonaceous species from different sources impact MAC, especially wood burning and other biomass sources (Laborde et al., 2013; Wu et al., 2021; Yuan et al., 2021; Zhang et al., 2020). Meteorological conditions, such as temperature, influence MAC (Srivastava et al., 2022), but this correlation varies by

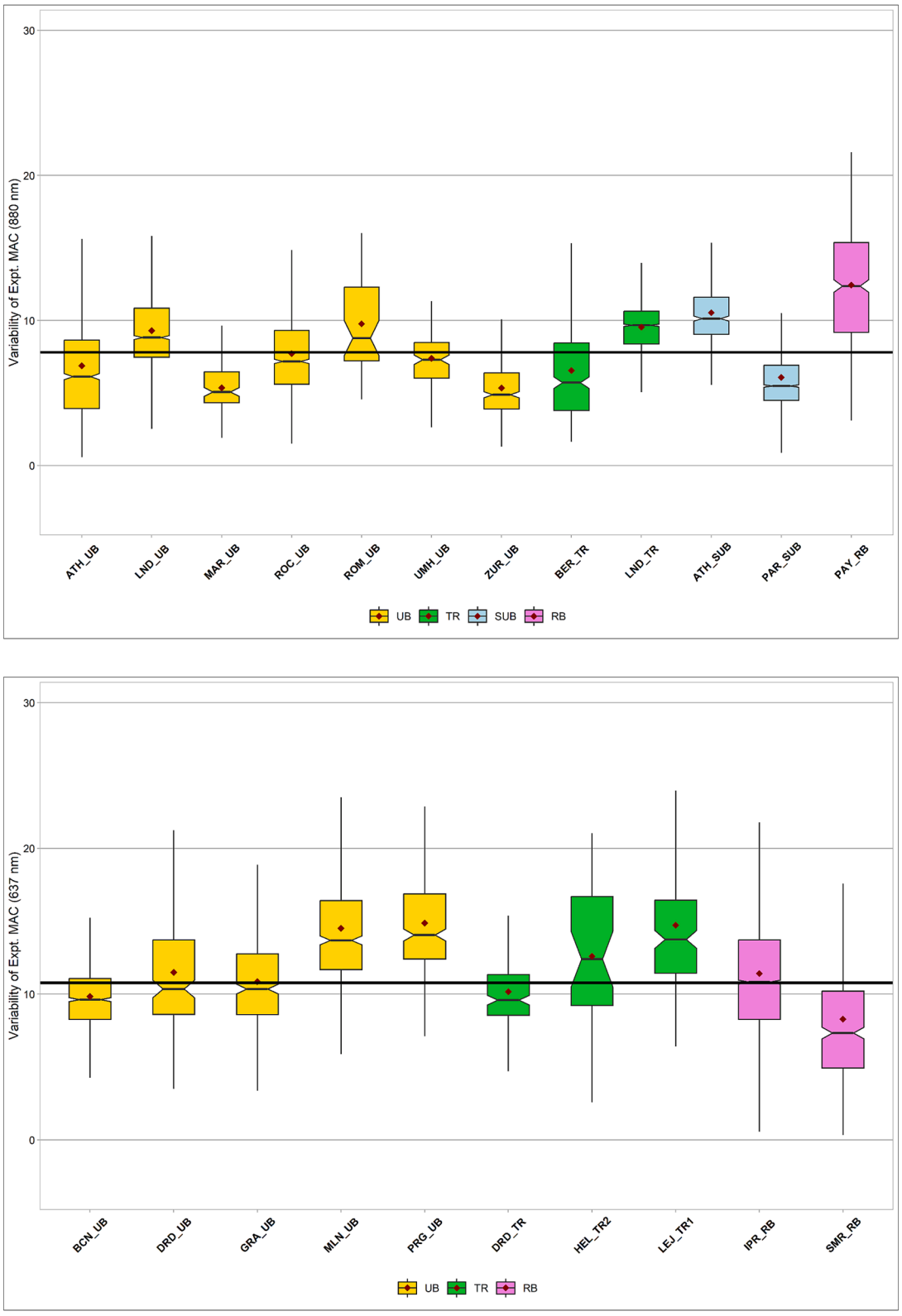

Fig. 3. Variability in experimental MAC at instrument-specific wavelengths (MAAP: 637 nm; AEs: 880 nm) across 22 sites categorized by site type (UB, urban background; SUB, suburban background; TR, traffic; RB, regional background). The upper panel correspond to AEs at 880 nm, while the lower panel correspond to MAAP instruments at 637 nm. The solid black line represents the total experimental median MAC for 12 AEs at 880 nm (7.8 ± 3.4 m^2 g^{-1}) and 10 MAAPs at 637 nm (10.6 ± 4.7 m^2 g^{-1}). Box-and-whisker plots depict the 25th and 75th quartiles, with the median indicated by a notched inner line. The mean is represented by the red points within the box plots. (For interpretation of the references to color in this figure legend, the reader is referred to the web version of this article.)

Table 2
Site-specific experimental MAC values for 22 monitoring sites obtained as the ratio of the b_{abs} to EC mass concentration at the instrument specific wavelengths AE 880 nm; MAAP 637 nm.

Sites	FAPs	Site-specific MAC [m^2g^{-1}], AE 880 nm; MAAP 637 nm	Number of observations
BCN_UB	MAAP	9.6 ± 2.6	1035
GRA_UB	MAAP	10.4 ± 3.3	391
ROC_UB	AE21	7.2 ± 2.8	1390
ATH_UB	AE33	6.1 ± 4.0	1244
MAR_UB	AE33	5.1 ± 1.7	120
DDW_UB	MAAP	10.4 ± 4.1	179
LND_UB	AE22	8.8 ± 2.6	1565
BER_TR	AE31-AE33	5.7 ± 3.5	350
ZUR_UB	AE33	4.9 ± 2.3	338
ROM_UB	AE33	8.8 ± 3.1	43
MLN_UB	MAAP	11.2 ± 6.5	1142
PRG_UB	MAAP	14.0 ± 3.7	296
UMH_UB	AE33	7.3 ± 2.1	136
HEL_TR2	MAAP	12.4 ± 4.7	38
LEJ_TR1	MAAP	13.8 ± 4.6	164
DDN_TR	MAAP	9.6 ± 2.6	181
LND_TR	AE22	9.7 ± 1.8	1856
ATH_SUB	AE33	10.1 ± 2.3	513
PAR_SUB	AE31-AE33	5.5 ± 3.0	2190
SMR_RB	MAAP	7.3 ± 4.7	432
IPR_RB	MAAP	10.8 ± 4.4	3945
PAY_RB	AE31-AE33	12.4 ± 4.1	494

region (Pandolfi et al., 2014). Coating materials, more prevalent in summer, and BC mixing states can significantly affect MAC values (Mbengue et al., 2021, 2020; Pandolfi et al., 2011, 2014; Zanatta et al., 2016; Zhao et al., 2021). Size-dependent MAC variations were also found to be source-specific (Bond and Bergstrom, 2006; Conrad and Johnson, 2019; Knox et al., 2009; Kondo et al., 2009).

3.3. Seasonality of the experimental mass absorption cross-section (MAC)

Fig. 5 presents the seasonal variation of MAC across different sites. As already noted, the MAC and its variation strongly depends on source-dependent eBC, physical properties as morphology, size, internal mixing and coating, among others. Other factors as the cross-sensitivity to scattering (Yus-Díez et al., 2021) could add additional uncertainty on the measured b_{abs} and consequently on the MAC. Yus-Díez et al. (2021) observed that high single scattering albedo (SSA) of the particles collected on the filter tape can cause an increase of C_0 (cross-sensitivity to scattering). However, according to Yus-Díez et al. (2021), no cross-sensitivity to scattering was observed in BCN_UB when contrasted with a regional background station (Montseny, MSY) and a mountaintop station (Montsec, MSA). This divergence was attributed to the consistently low SSA in BCN_UB. Such a pattern may potentially represent a general characteristic observable across our UB and TR-influenced sites (e.g. Laj et al., 2020). Thus, we consider that the cross-sensitivity to scattering could make marginal contribution and, in any event, falls within the overall uncertainty. A detailed description of the aforementioned physical factors causing the observed MAC seasonal cycles falls beyond the scope of this paper, primarily due to the necessity for additional detailed observations. These include, but are not limited to, comprehensive PM chemical speciation, single eBC particle characterization, scattering measurements, and concurrent monitoring of MAAP and AE measurements, for instance, as studied in Yus-Díez et al. (2021, 2022). Consequently, where feasible, we reference previously published works to interpret the observed cycles.

In addition, there has been reported different degrees of influence attributed to dust interactions on seasonal pattern of MAC in different geographical regions, such as Spain, Greece, Italy and Germany spanning from March to August (Athanasopoulou et al., 2016; Diapouli et al., 2016; Flentje et al., 2015; Gini et al., 2022; Gobbi et al., 2019; Pandolfi et al., 2014; Querol et al., 2019; Varga et al., 2014). Indeed, intense desert dust episodes (DDE) can affect the measured b_{abs} and consequently the calculated eBC concentrations. For example, Ripoll et al. (2015) have shown the effects of intense DDE on MAAP measurements performed at a high-altitude remote site in NE Spain (Montsec; MSA) where the concentrations of eBC are usually low. In fact, the mass absorption efficiency of dust particles is much lower compared to that of eBC (and especially in the visible range) and, consequently, an effect of dust on b_{abs} measurements during DDE can be significant where eBC concentrations are low. Moreover, the imaginary refractive index (indicating the absorptive properties of a particle) of dust particles is the highest in the UV spectral region and strongly decreases toward the visible/near-IR spectral range. The wavelengths used in this study for eBC determination, 637 nm (MAAP; visible) and 880 nm (AE; near-IR), are consequently less affected by dust absorption compared to the UV spectral region. Thus, at urban sites, where eBC is expected to dominate the b_{abs}, a significant effect of DDE on eBC concentrations is not expected. However, despite a potential minor impact of dust at 880 nm, it cannot be entirely ruled out, particularly when the cut-off for b_{abs} is PM_{10}. For this reason, we examined the influence of dust events on the calculated local MAC in Eastern Mediterranean Basin with frequent influences of dust (Sahara) such as ATH_SUB site using nephelometer data available in EBAS for Demokritos to detect dust days (using scattering Ångström exponent SAE < 1). Based on Fig. S3, the presence of 190 days of dust event observations did not apply a dominant influence on our dataset from 2017 to 2020. This comparison is evidenced by the calculated r^2 values when contrasting datasets that include all days, those excluding dust events, and those comprising only dust event observations. The exclusion of data related to dust events did not produce substantially different MAC values compared to those derived from the complete dataset. Moreover, as recently stated by Savadkoohi et al. (2023), particularly at UB sites such as BCN_UB, where eBC is expected to dominate the b_{abs}, the influence of sporadic desert dust on eBC concentrations is comparatively minimal over long timescales as evidenced by the correlation between eBC and NO_2 concentrations at BCN_UB.

Fig. 5 shows that the seasonal dependency at the UB sites followed different patterns, with elevated MAC values during the spring and summer or winter seasons depending on the site. ROC_UB exhibits significantly higher MAC values during the summertime compared to winter that might be attributed to local recreational wood burning (Masiol et al., 2019; Wang et al., 2012). At the ATH_UB site, monthly variations appear to be linked to the impact of BB, particularly during December to February in contrast to June to August. However, this variation does not attain statistical significance. GRA_UB showed significantly higher MAC values in winter that can be associated with open BB emissions of agricultural residues and domestic heating fueled by biomass sources in the rural area of Granada during the colder months (Lyamani et al., 2011; Titos et al., 2017). ZUR_UB showed low seasonality (i.e., not significant) compared to other Swiss sites that has been previously reported by Grange et al. (2020). Typically, summertime b_{abs} measures in Swiss sites have been reported to to be higher than those observed during wintertime. However, this seasonal variation has been reported to coincide with intra-instrumental variations, suggesting a plausible instrument artifact, possibly indicative of a slow degradation in sensitivity (Grange et al., 2020).

The BCN_UB site showed a seasonal fluctuation in MAC, characterized by comparatively elevated values in the summer. The results of statistical tests indicate a significant difference between summer and both spring and autumn. In contrast, the summer period has been previously characterized by a higher prevalence of available material for coating, such as seconday organic aerosol (SOA), as well as an increase in shipping emissions in BCN_UB (Pandolfi et al., 2020; Via et al., 2021). A more pronounced seasonal variation during winter and spring was observed at the MLN_UB site with statistically significant differences

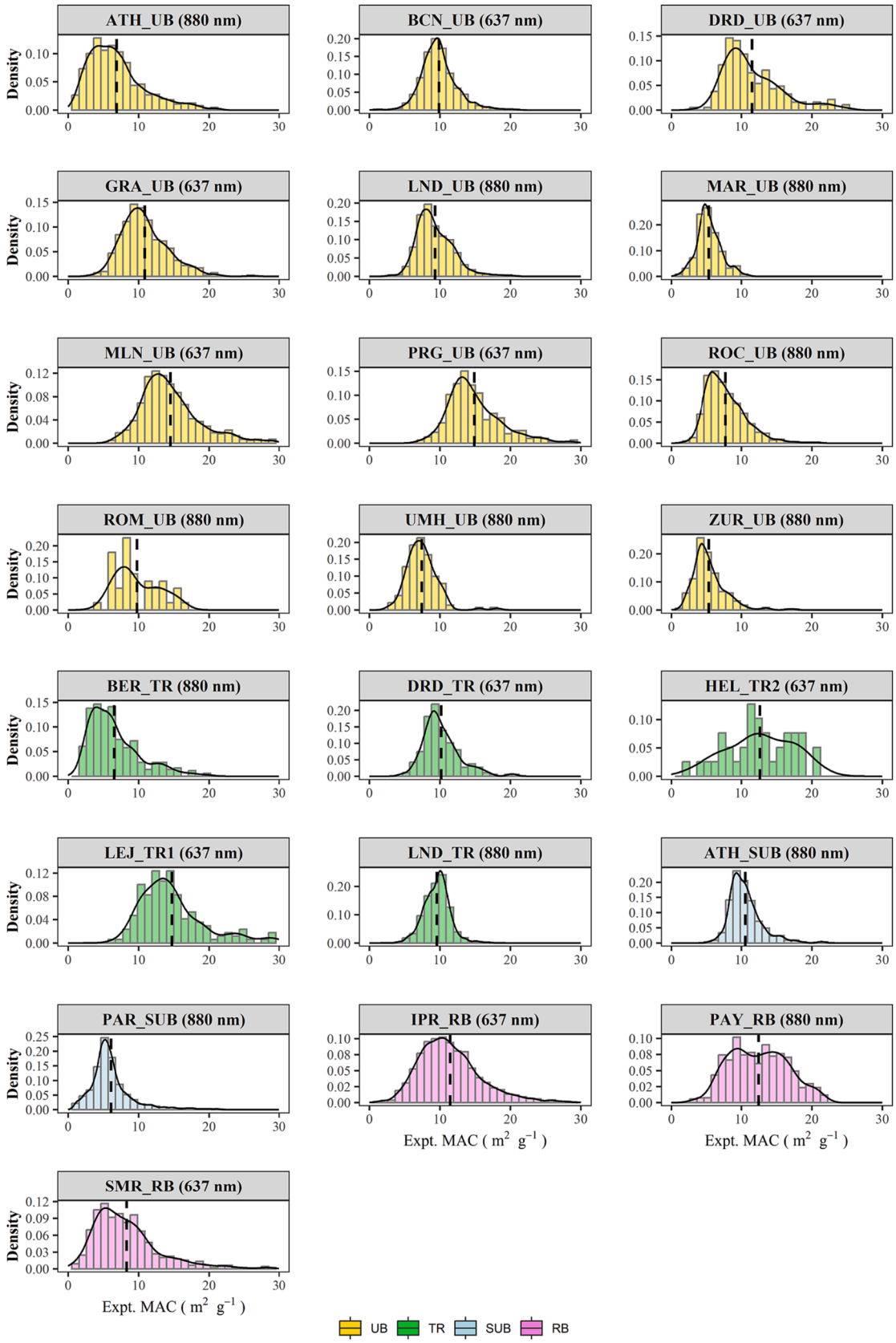

Fig. 4. Frequency distribution of experimental MAC for the whole available period. The color shading represents the type of site (UB, urban background; SUB, suburban background; TR, traffic; RB, regional background). The corresponding median MAC is shown in black sticks.

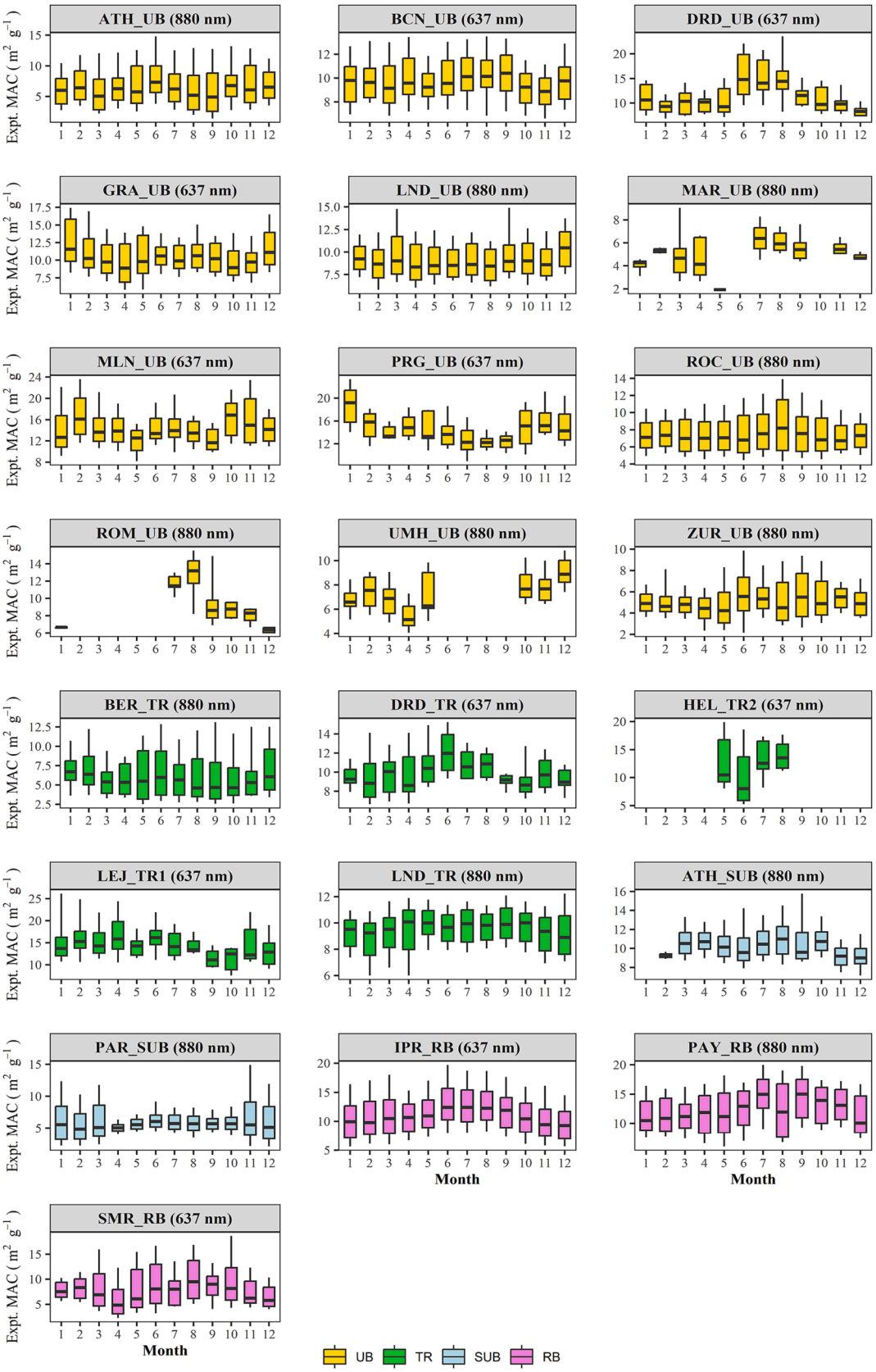

Fig. 5. Monthly variations in experimental MAC at 880 and 637 nm for 22 sites.The color shading represents the type of site (UB, urban background; SUB, suburban background; TR, traffic; RB, regional background). Box plots depict the 10th and 90th quantiles.

noted in winter vs. spring and summer vs. spring. However, Mousavi et al. (2019) has reported only slight seasonal changes in the MAC at 880 nm for the same site during three distinct seasons over 2017–2018. Their observation aligns with the outcomes of earlier studies by Zotter et al. (2017), indicating that MAC values are more influenced by the measurement location and site characteristics than by the season. At the PRG_UB site, the deviation observed in the fifth month is attributed to the annual biomass burning event that takes place during first May night in Czechia (Vodička et al., 2022). The increase in MAC during the tenth month is linked to the start of the heating season, typically occurring in mid-October.

Divergent seasonal patterns at the TR sites indicated data dispersion without uniform similarities across these sites. In BER_TR, as well as the ZUR_UB site, seasonal fluctuations were apparent in the MAC values. In Bern, a significant difference in the mean MAC was observed between the winter and autumn, as shown in Fig. 5. However, this difference was not found to be statistically significant in winter compared to the summer. The observed high temporal pattern of MAC in summer, as previously documented by Grange et al., (2020), can be attributed to higher b_{abs} measurements during the summer compared to winter. However, it is important to note that this pattern may not exclusively be linked to an increase in MAC but may also be pertinent to EC measurements at this particular site. Considering the four TR sites in this study, the seasonal pattern was found to be more pronounced at LND_TR as shown in Fig. 5. The statistical analysis revealed significant differences between winter and the other seasons at this site. This pattern aligns with the observations of Ciupek et al. (2021) who has documented a clear seasonal variation with a reduction in MAC values during the winter. This winter decrease in MAC has been reported to be associated with the changes to the SOA concentration and a combination of other changes in the physical properties of atmospheric aerosols (Ciupek et al., 2021; Zhang et al., 2018). The DRD_TR and LEJ_TR1 sites showed a more pronounced seasonal pattern of MAC during summer compared to winter. These sites have previously been categorized as sites strongly influenced by traffic, sharing a similar source influence (Sun et al., 2019). Monthly variation of experimental MAC observed in IPR_RB, exhibited a similarity to the seasonal pattern of b_{abs} and EC mass concentration, as observed by Zanatta et al. (2016) at this site. IPR_RB, which was reported to be strongly affected by anthropogenic emissions, generally had higher EC concentrations compared to other RB sites (Sandrini et al., 2014). Our results found a statistically significant difference in the mean of experimental MAC between winter and summer with high values observed during the summer. A comparable and statistically significant monthly variation in summer is also evident at SMR_RB site.

In contrast, the ATH_SUB and PAR_SUB sites showed distinct monthly variations. PAR_SUB exhibited the lowest MAC values during the spring months, while reaching peak levels during autumn and winter, a trend that can be linked to increased residential wood burning emissions during colder periods (Zhang et al., 2019). At ATH_SUB, MAC exhibited a pronounced seasonal dependency, which was statistically significant between summer vs. winter with higher MAC in summer. This may be attributed to the formation of secondary sulfate and organic aerosols during the summer which results in coatings of the MAC, commonly referred to as lensing effect (Pandolfi et al., 2018). In other sites (i.e., ROM_UB, MAR_UB, and HEL_TR2), the number of observations was insufficient to characterize the temporal variability of the corresponding region. It limits the interpretation of monthly variations and the identification of consistent seasonal patterns. However, MAR_UB demonstrated a statistically significant difference in experimental MAC between winter and summer, considering the available number of observations. Overall, the results of the mean analysis methods employed to assess the significance of differences in experimental MAC for various seasons, using both parametric (ANOVA) and non-parametric (Kruskal-Wallis) tests, revealed distinct patterns of p-values across 22 sites. Detailed p-values for all sites are provided in Table S1, while Fig. S4 visually depicts the difference in the mean experimental MAC in different seasons, presented with a 95 % confidence interval.

3.4. Impact of chosen MAC value on estimation of eBC mass concentration

Considering the observed variations in MAC values among the monitoring sites and the presence of strong seasonal dependency, NeBC mass concentrations were recalculated from b_{abs} at 637 and 880 nm. This correction method was performed using median MAC from 22 sites, site-specific MAC, and site-specific rolling MAC (regression). Subsequently, the corrected eBC mass concentrations obtained through these methods were named: *MeBC* (using median MAC), *LeBC* (local MAC), and *ReBC* (Rolling MAC) respectively. Fig. S5 shows the monthly variations of NeBC, MeBC, LeBC, and ReBC mass concentrations. The difference is seen to be quasi constant throughout the months. This pattern was consistently observed across all other sites, showing variations and relative percentage differences (RPD%) in both MAAP and AEs measurements. RPD% were computed to quantify the degree of variability between NeBC and ReBC, as well as between NeBC and MeBC. The sites PRG_UB, ROM_UB, UMH_UB, MLN_UB, DRD_UB, and LND_TR showed the highest RPD% in descending order.

The variation estimated to reach up to 70 % when comparing NeBC to ReBC. Moreover, it is important to note that employing MeBC derived from median MAC at sites without EC measurements may introduce certain errors. The RPD of NeBC and MeBC varied within the range of 26–67 % (see Fig. S5). In addition, the mean absolute error (MAE) values of MeBC and ReBC are presented in Table S2. As shown in Fig. S5, the corrected eBC mass concentrations were highly sensitive to the uncertainty and variability associated with the chosen MAC value. Especially, LeBC aligned more closely with the ReBC. Nevertheless, MeBC exhibited a substitution that occasionally coincides with the rolling and site-specific approaches; conversely, in certain cases, it aligns either below or above the results of the other two methods, reflecting the relatively high uncertainty in use of constant MAC value. However, these corrected eBC values consistently remained lower than the NeBC mass concentrations. Consequently, it can be inferred that employing a constant MAC value for different sites within the AQMNs can yield misleading results. This highlights the critical importance of employing site-specific MAC to mitigate the potential inaccuracies produced by NeBC mass concentration.

Among the various approaches employed here for MAC estimation, the site-specific and rolling approaches were found to be more robust. The rolling and site-specific methods could consider the physical–chemical attributes of each site over a period of time to estimate the eBC mass concentration. Furthermore, as depicted in Fig. S5, median values occasionally resulted in an overestimation or underestimation of the eBC mass concentration when compared to the values derived from the site-specific and rolling approaches. It is worth noting that not all monitoring sites are able to adopt these methods due to the lack of EC measurements. However, it is of prime interest to refine the estimation of eBC mass concentration within research studies, as it may contribute to significantly-improved assessments of the climate and AQ implications associated with BC particles.

3.5. eBC mass concentrations and MAC trend analysis

MAC values were not only dependent on the site and/or season but can also have long-term changes. Studying long-term trends of experimental MAC from prolonged monitoring measurements are beneficial for robust MAC determination. Therefore, long-time series of NeBC and EC mass concentration data from monitoring sites (specifically BCN_UB, IPR_RB, ROC_UB, PAR_SUB, and ZUR_UB) were analyzed with Theil-Sen slope regression for trend analysis (Carslaw and Ropkins, 2012). There are very few published studies on the long-term trends of experimental MAC at sites measuring EC, such as Ciupek et al. (2021). Fig. S6 shows

statistically significant decreasing trends in eBC mass concentration using nominal MAC across all studied sites over time. These decreasing eBC trends were consistent with previous studies documenting long-term eBC trends in Europe and the US (Collaud Coen et al., 2020; Jafar and Harrison, 2021; Luoma et al., 2021; Masiol et al., 2018; Savadkoohi et al., 2023). Similar decreasing trends in EC concentrations were observed aligned with previous findings in other European regions. However, there are studies reporting an increasing trend in EC concentration such as a rural site in the UK (Ciupek et al., 2021).

PAR_SUB (−7.64 %/year) showed the most pronounced and statistically significant decreasing trends in NeBC mass concentration. This declining pattern corresponded consistently with the statistically significant downward trend observed in EC mass concentration at this site. However, a modestly increasing trend (1.47 %/year) was observed in the experimental MAC. This observation could potentially be attributed to the relatively stable trend in eBC wood burning concentrations that can vary depending on factors like the source of the wood, burning conditions, and a significant decreasing trend of eBC traffic at the PAR_SUB site, as reported by Zhang et al. (2019). Upon applying the rolling MAC approach, a statistically significant decreasing trend (−6.28 %/year) was observed for ReBC, although it was generally lower than the trend observed for NeBC concentration.

At the ZUR_UB site, a modest decline in NeBC mass concentrations (−1.9 %/year) was detected. Conversely, EC mass concentration exhibited a statistically significant downward trend (−5.73 %/year) at this site. The experimental MAC displayed a slight increase with a slope of 1.57 %/year. As for PAR_SUB, this could potentially be linked to the wood burning emissions decreasing at a lower rate in comparison to the decline observed in traffic emissions at this site, a phenomenon previously discussed by Grange et al. (2020) for Zürich. These findings underscore the significance of considering specific emission sources and their respective trends as important factors in understanding the long-term variations in MAC values. By applying the rolling MAC, a pronounced descending trend of ReBC was observed with annual decrease of −4.57 % over the years 2012 to 2022.

Among all sites, the ROC_UB site showed a statistically significant decreasing trend in NeBC concentrations at a rate of −3.76 % per year. The estimated experimental MAC demonstrated a declining trend over time with a statistically significant slope of −3.76 %/year. In contrast, the EC concentration exhibited a slight increase with a slope of 1.2 %/year although not statistically significant. However, when employing the rolling MAC, almost no statistically significant trend was observed for ReBC at ROC_UB (0.56 %/year). This difference might be the result of changes in emissions, evolving regulatory measures, and the potential decline in wood-burning emissions over the years 2009–2022, suggesting a possible change in EC sources as a plausible explanation for the declining trend in experimental MAC.

At the IPR_RB site, a significant declining trend was observed in both NeBC (−3.58 %/year) and EC concentrations (−3.53 %/year). These trends contradicted the FAPs measurement trend for years prior to 2010, which was reported by Putaud et al. (2014) over the 2004–2010 period. Interestingly, MAC displayed a distinct behavior at this site, exhibiting a slight increasing but not significant trend with a slope of 0.59 %/year. This finding suggests that coatings might contribute to the elevation of MAC to some degree at this site (Kalbermatter et al., 2022), influenced by pollution from the Po Valley (Zanatta et al., 2016). Furthermore, ReBC mass concentration also demonstrated a statistically significant trend (−3.25 %/year) at IPR_RB.

At the BCN_UB site, both NeBC (−4.95 %/year) and EC mass concentrations (−3.69 %/year) displayed statistically significant decreasing trends. This trend in NeBC concentration aligns with a recent study by Savadkoohi et al. (2023) who reported a decrease of −4.7 % yr^{-1} between 2010 and 2020 at the same site. Additionally, the observed trend is consistent with the other studies that reported a significant NeBC decrease (−18 %) from 2014 to 2018 at the same site (Via et al., 2021), suggesting the influence of traffic emission reduction policies as a possible cause (Carnerero et al., 2021). Interestingly, the decreasing trend of experimental MAC at BCN_UB was not statistically significant, indicating a slight decrease over the measurement period. Furthermore, our result identified a significant decreasing trend in the ReBC mass concentration, with a slightly different slope of −4.62 %/year between 2010 and 2020.

4. Conclusions and recommendations

The primary aims of this study were i) to establish a consistent estimation of normalized equivalent black carbon mass concentration (eBC) from different FAPs in different environments and ii) to examine the variability of mass absorption cross-section (MAC) and iii) to refine methodologies for the calculation of site-specific eBC mass concentration. This investigation was performed by analyzing the long-term changes in experimental MAC across 22 sites, using co-located observations of absorption coefficients (b_{abs}) from FAPs and elemental carbon (EC). The resulting median MAC values were as follows: 7.8 ± 3.4 m^2 g^{-1} at 880 nm from 12 AEs and 10.6 ± 4.7 m^2 g^{-1} at 637 nm from 10 MAAPs. The median MAC from MAAP reported here closely aligns with the MAC value of 10.0 m^2 g^{-1} recommended by ACTRIS based on previous study from Zanatta et al. (2016).

The difference between the nominal MAC employed in FAPs and the median MAC values reported in this study, was very pronounced in the case of MAAP that uses a MAC of 6.6 m^2 g^{-1} at 637 nm for reporting eBC concentrations. Consequently, nominal eBC (NeBC) concentrations derived from MAAP are overestimated approximately 40 % when compared to the median MAC of 10.6 m^2 g^{-1} for eBC calculation. Contrastingly, for AE33 instruments, the nominal MAC value at 880 nm (7.77 m^2 g^{-1}) closely aligns with the median MAC reported in this study (7.8 m^2 g^{-1}). Nonetheless, the primary source of uncertainty in the reported nominal eBC values from AE33 instruments arises from the utilization of a filter multiple-scattering parameter (C_0) with a value of 1.39 in the AE33 software. This value is approximately 45 % lower than the value of 2.44 selected for harmonizing absorption measurements from AE33 instruments, as noted in previous studies (e.g., Savadkoohi et al., 2023). We performed a comparison between the nominal eBC mass concentrations provided by FAPs and the concentrations of eBC obtained using various experimental MAC values, including median MAC calculated for the 22 sites, site-specific MAC, and rolling MAC. NeBC consistently exhibited an overestimation ranging from 40 % to 80 %.

Given the observed strong temporal and spatial variability of the experimental MAC values reported here, we conclude that having a local estimation of the MAC from simultaneous b_{abs} and EC measurements is the best approach to reduce the eBC uncertainty. Moreover, considering the temporal variability of the MAC, the rolling MAC can be considered as the most appropriate conversion factor to estimate eBC concentrations from optical measurements. In fact, in this case the eBC concentrations are continuously normalized to the concentrations of EC for which a reference method exists (EN16909, 2017). This long-term continuous normalization is also useful when the trends of eBC are analyzed. Indeed, the long-term trend analysis reported here revealed that the trend of eBC obtained using any constant MAC value (nominal, local or median MAC) might lead to misleading interpretation of the eBC trend if any trend in MAC is also observed. Thus, the long-term trends of eBC explicitly mirror the EC trends only when the rolling MAC is used.

Therefore, investigating a site-specific MAC is recommended, when and where possible, instead of relying on the nominal MAC values provided by instrument manufacturers. To strengthen the applicability of site-specific MAC values for improved estimation of eBC mass concentrations, this study recommends the use of co-located measurements of b_{abs} and EC mass concentrations by expanding monitoring networks to include regular EC sampling and periodically using EC measurements to obtain rolling MAC. Other researchers also recommended this approach to effectively employ b_{abs} data for improved analysis and interpretation (Ciupek et al., 2021; Contini et al., 2018; Helin et al.,

2018; Grange et al., 2020; Salako et al., 2012). This approach addresses two significant aspects. Firstly, it enables a more accurate estimation of the mass concentration of absorbing particles for AQ assessment. Secondly, it facilitates the experimental determination of MAC for climate-related studies including aerosol direct radiative forcing calculations. However, whenever EC observations are unavailable, we recommend applying the median MAC value of 10.6 m^2 g^{-1} obtained in this work when b_{abs} is provided by MAAP at 637 nm and the MAC value of 7.8 m^2 g^{-1} when harmonized b_{abs} is provided by aethalometers at 880 nm

CRediT authorship contribution statement

Marjan Savadkoohi: Writing – review & editing, Writing – original draft, Visualization, Validation, Software, Resources, Methodology, Investigation, Funding acquisition, Formal analysis, Data curation. **Marco Pandolfi:** Writing – review & editing, Validation, Supervision, Resources, Methodology, Funding acquisition, Conceptualization. **Olivier Favez:** Writing – review & editing, Validation. **Jean-Philippe Putaud:** Writing – review & editing, Validation, Data curation. **Konstantinos Eleftheriadis:** Writing – review & editing, Data curation. **Markus Fiebig:** Writing – review & editing, Data curation. **Philip K. Hopke:** Writing – review & editing, Validation. **Paolo Laj:** Writing – review & editing, Validation. **Alfred Wiedensohler:** Writing – review & editing, Validation. **Lucas Alados-Arboledas:** Data curation. **Susanne Bastian:** Data curation. **Benjamin Chazeau:** Data curation. **Álvaro Clemente María:** Data curation. **Cristina Colombi:** Data curation. **Francesca Costabile:** Data curation. **David C. Green:** Data curation. **Christoph Hueglin:** Writing – review & editing, Data curation. **Eleni Liakakou:** Data curation. **Krista Luoma:** Data curation. **Stefano Listrani:** Data curation. **Nikos Mihalopoulos:** Data curation. **Nicolas Marchand:** Data curation. **Griša Močnik:** Writing – review & editing, Validation. **Jarkko V. Niemi:** Writing – review & editing, Data curation. **Jakub Ondráček:** Data curation. **Jean-Eudes Petit:** Data curation. **Oliver V. Rattigan:** Data curation. **Cristina Reche:** Data curation. **Hilkka Timonen:** Writing – review & editing, Data curation. **Gloria Titos:** Writing – review & editing, Data curation. **Anja H. Tremper:** Data curation. **Stergios Vratolis:** Data curation. **Petr Vodička:** Data curation. **Eduardo Yubero Funes:** Data curation. **Naděžda Zíková:** Data curation. **Roy M. Harrison:** Writing – review & editing, Validation. **Tuukka Petäjä:** Writing – review & editing, Funding acquisition, Data curation. **Andrés Alastuey:** Writing – review & editing, Writing – original draft, Validation, Supervision, Resources, Methodology, Funding acquisition, Conceptualization. **Xavier Querol:** Writing – review & editing, Validation, Supervision, Resources, Funding acquisition.

Declaration of competing interest

Griša Močnik is employed by Haze Instruments d.o.o., the manufacturer of the aerosol instrumentation.

Data availability

The time series of eBC mass concentrations and absorption coefficients of 22 studied sites are available online at (https://doi.org/10.5281/zenodo.7982201). Any requests for materials should be addressed to the corresponding author, M. Savadkoohi.

Acknowledgments

This work was funded and supported within the framework of the Research Infrastructures Services Reinforcing AQ Monitoring Capacities in European Urban & Industrial AreaS (RI-URBANS) project. The RI-URBANS project (https://riurbans.eu/, contract 101036245), is a European H2020-Green Deal initiative that aims to provide comprehensive tools for the measurement and analysis of advanced AQ parameters (RI-URBANS, 2020). These parameters include eBC, ultrafine particles, and oxidative potential in urban environments, which will consequently allow for the enhanced assessment of AQ policies. RI-URBANS is implementing the ACTRIS (https://www.actris.eu/) strategy for the development of services for improving air quality in Europe.

The authors would like to also thank the support from "Agencia Estatal de Investigación" from the Spanish Ministry of Science and Innovation under the project CAIAC (PID2019-108990RB-I00), AIRPHONEMA (PID2022-142160OB-I00), and the Generalitat de Catalunya (AGAUR, SGR-447). M. Savadkoohi would like to thank the Spanish Ministry of Science and Innovation for her FPI grant (PRE-2020-095498). This study is also partly funded by the National Institute for Health Research (NIHR) Health Protection Research Unit in Environmental Exposures and Health, a partnership between UK Health Security Agency (UKHSA) and Imperial College London, and the UK Natural Environment Research Council. The views expressed are those of the author(s) and not necessarily those of the NIHR, UKHSA or the Department of Health and Social Care. The work in Helsinki and Hyytiälä is supported by Academy of Finland flagship "Atmosphere and Climate Competence Center (ACCC), project numbers 337549, 337552, 334792, 328616, 345510 and the Technology Industries of Finland Centennial Foundation Urban Air Quality 2.0 project and European Commission via FOCI-project (grant number 101056783). The work performed in Rome (IT) was supported by ARPA Lazio, the regional Environmental Protection Agency. Measurements at Granada urban station were possible thanks to MCIN/AEI/10.13039/501100011033 and NextGenerationEU/PRTR under the projects PID2020-120015RB-I00 and PID2021-128757OB-I00, ACTRIS-España (CGL2017-90884REDT), and University of Granada Plan Propio through Excellence Research Unit Earth Science and Singular Laboratory AGORA (LS2022-1). Partial support of this work by the project "PANhellenic infrastructure for Atmospheric Composition and climatE change" (MIS 5021516) which is implemented under the Action "Reinforcement of the Research and Innovation Infrastructure", funded by the Operational Programme "Competitiveness, Entrepreneurship and Innovation" (NSRF 2014-2020) and co-financed by Greece and the European Union (European Regional Development Fund). Partial funding was obtained by Slovenian ARRS/ARIS program P1-0385. Partial support for operating stations in France is received by ACTRIS-FR supported by French Ministery for research and Education and by France2030 initiative under project ANR-21-ESRE-0013. Elche data were possible thanks to the support of European Union NextGenerationEU/PRTR" (CAMBIO project, ref. TED2021-131336B-I00) and by the Valencian Regional Government (Generalitat Valenciana, CIAICO/2021/280 research project). This research was supported by the Ministry of Education, Youth and Sports of the Czech Republic within the Large Research Infrastructure Support Project - ACTRIS Participation of the Czech Republic (ACTRIS-CZ LM2023030).

Appendix A. Supplementary material

Supplementary data to this article can be found online at https://doi.org/10.1016/j.envint.2024.108553.

References

ACTRIS-ECAC. Recommendations, guidelines, standard operating procedures and scientific articles for aerosol in-situ measurements. https://www.actris-ecac.eu/measurement-guidelines.html (accessed 8.31.22).

Asmi, E., Backman, J., Servomaa, H., Virkkula, A., Gini, M.I., Eleftheriadis, K., Müller, T., Ohata, S., Kondo, Y., Hyvärinen, A., 2021. Absorption instruments inter-comparison campaign at the Arctic Pallas station. Atmos. Meas. Tech. 14, 5397–5413. https://doi.org/10.5194/amt-14-5397-2021.

Athanasopoulou, E., Protonotariou, A., Papangelis, G., Tombrou, M., Mihalopoulos, N., Gerasopoulos, E., 2016. Long-range transport of Saharan dust and chemical transformations over the Eastern Mediterranean. Atmos. Environ. 140, 592–604. https://doi.org/10.1016/j.atmosenv.2016.06.041.

Barreira, M.F., Helin, A., Aurela, M., Teinila, K., Friman, M., Kangas, L., Niemi, V., Portin, H., Kousa, A., Pirjola, L., Ronkko, T., Saarikoski, S., Timonen, H., 2021. In-depth characterization of submicron particulate matter inter-annual variations at a

street canyon site in northern Europe. Atmos. Chem. Phys. 21, 6297–6314. https://doi.org/10.5194/acp-21-6297-2021.
Bond, T.C., Bergstrom, R.W., 2006. Light absorption by carbonaceous particles: an investigative review. Aerosol Sci. Technol. 40, 27–67. https://doi.org/10.1080/02786820500421521.
Bond, T.C., Doherty, S.J., Fahey, D.W., Forster, P.M., Berntsen, T., Deangelo, B.J., Flanner, M.G., Ghan, S., Kärcher, B., Koch, D., Kinne, S., Kondo, Y., Quinn, P.K., Sarofim, M.C., Schultz, M.G., Schulz, M., Venkataraman, C., Zhang, H., Zhang, S., Bellouin, N., Guttikunda, S.K., Hopke, P.K., Jacobson, M.Z., Kaiser, J.W., Klimont, Z., Lohmann, U., Schwarz, J.P., Shindell, D., Storelvmo, T., Warren, S.G., Zender, C.S., 2013. Bounding the role of black carbon in the climate system: a scientific assessment. J. Geophys. Res. Atmos. 118, 5380–5552. https://doi.org/10.1002/jgrd.50171.
Cao, J., Zhu, C., Ho, K., Han, Y., Shen, Z., Zhan, C., Zhang, J., 2015. Light attenuation cross-section of black carbon in an urban atmosphere in northern China. Particuology 18, 89–95. https://doi.org/10.1016/j.partic.2014.04.011.
Carnerero, C., Rivas, I., Reche, C., Pérez, N., Alastuey, A., Querol, X., 2021. Trends in primary and secondary particle number concentrations in urban and regional environments in NE Spain. Atmos. Environ. 244 https://doi.org/10.1016/j.atmosenv.2020.117982.
Carslaw, D.C., Ropkins, K., 2012. Openair - an r package for air quality data analysis. Environ. Model. Softw. 27–28, 52–61. https://doi.org/10.1016/j.envsoft.2011.09.008.
Casquero-Vera, J.A., Lyamani, H., Titos, G., Minguillón, M.C., Dada, L., Alastuey, A., Querol, X., Petäjä, T., Olmo, F.J., Alados-Arboledas, L., 2021. Quantifying traffic, biomass burning and secondary source contributions to atmospheric particle number concentrations at urban and suburban sites. Sci. Total Environ. 768 https://doi.org/10.1016/j.scitotenv.2021.145282.
Cavalli, F., Putaud, J.P., 2010. Toward a standardized thermal-optical protocol for measuring atmospheric organic and elemental carbon: the eusaar protocol. ACS, Div. Environ. Chem. - Prepr. Ext. Abstr. 48, 443–446.
Cho, C., Kim, S.W., Lee, M., Lim, S., Fang, W., Gustafsson, Ö., Andersson, A., Park, R.J., Sheridan, P.J., 2019. Observation-based estimates of the mass absorption cross-section of black and brown carbon and their contribution to aerosol light absorption in East Asia. Atmos. Environ. 212, 65–74. https://doi.org/10.1016/j.atmosenv.2019.05.024.
Ciupek, K., Quincey, P., Green, D.C., Butterfield, D., Fuller, G.W., 2021. Challenges and policy implications of long-term changes in mass absorption cross-section derived from equivalent black carbon and elemental carbon measurements in London and south-East England in 2014–2019. Environ. Sci. Process. Impacts 23, 1949–1960. https://doi.org/10.1039/d1em00200g.
Collaud Coen, M., Weingartner, E., Apituley, A., Ceburnis, D., Fierz-Schmidhauser, R., Flentje, H., Henzing, J.S., Jennings, S.G., Moerman, M., Petzold, A., Schmid, O., Baltensperger, U., 2010. Minimizing light absorption measurement artifacts of the aethalometer: evaluation of five correction algorithms. Atmos. Meas. Tech. 3, 457–474. https://doi.org/10.5194/amt-3-457-2010.
Collaud Coen, M., Andrews, E., Lastuey, A., Petkov Arsov, T., Backman, J., Brem, B.T., Bukowiecki, N., Couret, C., Eleftheriadis, K., Flentje, H., Fiebig, M., Gysel-Beer, M., Hand, J.L., Hoffer, A., Hooda, R., Hueglin, C., Joubert, W., Keywood, M., Eun Kim, J., Kim, S.W., Labuschagne, C., Lin, N.H., Lin, Y., Lund Myhre, C., Luoma, K., Lyamani, H., Marinoni, A., Mayol-Bracero, O.L., Mihalopoulos, N., Pandolfi, M., Prats, N., Prenni, A.J., Putaud, J.P., Ries, L., Reisen, F., Sellegri, K., Sharma, S., Sheridan, P., Patrick Sherman, J., Sun, J., Titos, G., Torres, E., Tuch, T., Weller, R., Wiedensohler, A., Zieger, P., Laj, P., 2020. Multidecadal trend analysis of in situ aerosol radiative properties around the world. Atmos. Chem. Phys. 20, 8867–8908. https://doi.org/10.5194/acp-20-8867-2020.
Conrad, B.M., Johnson, M.R., 2019. Mass absorption cross-section of flare-generated black carbon: variability, predictive model, and implications. Carbon N. Y. 149, 760–771. https://doi.org/10.1016/j.carbon.2019.04.086.
Contini, D., Vecchi, R., Viana, M., 2018. Carbonaceous aerosols in the atmosphere. Atmosphere (Basel) 9, 1–8. https://doi.org/10.3390/atmos9050181.
Cuesta-Mosquera, A., Mocnik, G., Drinovec, L., Müller, T., Pfeifer, S., Minguillon, M.C., Briel, B., Buckley, P., Dudoitis, V., Fernández-García, J., Fernandez-Amado, M., De Brito, J.F., Riffault, V., Flentje, H., Heffernan, E., Kalivitis, N., Kalogridis, A.C., Keernik, H., Marmureanu, L., Luoma, K., Marinoni, A., Pikridas, M., Schauer, G., Serfozo, N., Servomaa, H., Titos, G., Yus-Diez, J., Zioła, N., Wiedensohler, A., 2021. Intercomparison and characterization of 23 aethalometers under laboratory and ambient air conditions: procedures and unit-to-unit variabilities. Atmos. Meas. Tech. 14, 3195–3216. https://doi.org/10.5194/amt-14-3195-2021.
Diapouli, E., Manousakas, M.I., Vratolis, S., Vasilatou, V., Pateraki, S., Bairachtari, K.A., Querol, X., Amato, F., Alastuey, A., Karanasiou, A.A., Lucarelli, F., Nava, S., Calzolai, G., Gianelle, V.L., Colombi, C., Alves, C., Custódio, D., Pio, C., Spyrou, C., Kallos, G. B., Eleftheriadis, K., 2016. AIRUSE-LIFE+: Estimation of natural source contributions to urban ambient air PM 10 and PM 2. 5 concentrations in Southern Europe. Implications to compliance with limit values. 1–25. doi: 10.5194/acp-2016-781.
Diapouli, E., Kalogridis, A.C., Markantonaki, C., Vratolis, S., Fetfatzis, P., Colombi, C., Eleftheriadis, K., 2017. Annual variability of black carbon concentrations originating from biomass and fossil fuel combustion for the suburban aerosol in Athens, Greece. Atmosphere (Basel) 8. https://doi.org/10.3390/atmos8120234.
Drinovec, L., Močnik, G., Zotter, P., Prévôt, A.S.H., Ruckstuhl, C., Coz, E., Rupakheti, M., Sciare, J., Müller, T., Wiedensohler, A., Hansen, A.D.A., 2015. The "dual-spot" Aethalometer: an improved measurement of aerosol black carbon with real-time loading compensation. Atmos. Meas. Tech. 8, 1965–1979. https://doi.org/10.5194/amt-8-1965-2015.
European Committee for Standardisation, 2017. EN 16909:2017, Ambient Air – Measurement of Elemental Carbon (EC) and Organic Carbon (OC) Collected on Filters. CEN, Brussels.
Flentje, H., Briel, B., Beck, C., Collaud Coen, M., Fricke, M., Cyrys, J., Gu, J., Pitz, M., Thomas, W., 2015. Identification and monitoring of Saharan dust: an inventory representative for South Germany since 1997. Atmos. Environ. 109, 87–96. https://doi.org/10.1016/j.atmosenv.2015.02.023.
Gini, M., Manousakas, M., Karydas, A.G., Eleftheriadis, K., 2022. Mass size distributions, composition and dose estimates of particulate matter in Saharan dust outbreaks. Environ. Pollut. 298, 118768 https://doi.org/10.1016/j.envpol.2021.118768.
Gobbi, G.P., Barnaba, F., Di Liberto, L., Bolignano, A., Lucarelli, F., Nava, S., Perrino, C., Pietrodangelo, A., Basart, S., Costabile, F., Dionisi, D., Rizza, U., Canepari, S., Sozzi, R., Morelli, M., Manigrasso, M., Drewnick, F., Struckmeier, C., Poenitz, K., Wille, H., 2019. An inclusive view of Saharan dust advections to Italy and the Central Mediterranean. Atmos. Environ. 201, 242–256. https://doi.org/10.1016/j.atmosenv.2019.01.002.
Grange, S., Lötscher, H., Fischer, A., Emmenegger, L., Hueglin, C., 2020. Evaluation of equivalent black carbon source apportionment using observations from Switzerland between 2008 and 2018. Atmos. Meas. Tech. 13, 1867–1885. https://doi.org/10.5194/amt-13-1867-2020.
Gundel, L.A., Dod, R.L., Rosen, H., Novakov, T., 1984. The relationship between optical attenuation and black carbon concentration for ambient and source particles. Sci. Total Environ. 36, 197–202. https://doi.org/10.1016/0048-9697(84)90266-3.
Helin, A., Niemi, J.V., Virkkula, A., Pirjola, L., Teinilä, K., Backman, J., Aurela, M., Saarikoski, S., Rönkkö, T., Asmi, E., Timonen, H., 2018. Characteristics and source apportionment of black carbon in the Helsinki metropolitan area, Finland. Atmos. Environ. 190, 87–98. https://doi.org/10.1016/j.atmosenv.2018.07.022.
Ivančič, M., Gregorič, A., Lavrič, G., Alföldy, B., Ježek, I., Hasheminassab, S., Pakbin, P., Ahangar, F., Sowlat, M., Boddeker, S., Rigler, M., 2022. Two-year-long high-time-resolution apportionment of primary and secondary carbonaceous aerosols in the Los Angeles Basin using an advanced total carbon–black carbon (TC-BC(Λ)) method. Sci. Total Environ. 848 https://doi.org/10.1016/j.scitotenv.2022.157606.
Jafar, H.A., Harrison, R.M., 2021. Spatial and temporal trends in carbonaceous aerosols in the United Kingdom. Atmos. Pollut. Res. 12, 295–305. https://doi.org/10.1016/j.apr.2020.09.009.
Janssen, Nicole, A.H., Gerlofs-Nijland, Miriam E, Lanki, Timo, Salonen, Raimo O, Cassee, Flemming, et al., 2012. Health effects of black carbon. World Health Organization. Regional Office for Europe. https://iris.who.int/handle/10665/352615.
Janssen, N.A.H., Hoek, G., Simic-Lawson, M., Fischer, P., van Bree, L., Brink, H.T., Keuken, M., Atkinson, R.W., Ross Anderson, H., Brunekreef, B., Cassee, F.R., 2011. Black carbon as an additional indicator of the adverse health effects of airborne particles compared with pm10 and pm2.5. Environ. Health Perspect. 119, 1691–1699. https://doi.org/10.1289/ehp.1003369.
Kalbermatter, D.M., Močnik, G., Drinovec, L., Visser, B., Röhrbein, J., Oscity, M., Weingartner, E., Hyvärinen, A.P., Vasilatou, K., 2022. Comparing black-carbon-and aerosol-absorption-measuring instruments-a new system using lab-generated soot coated with controlled amounts of secondary organic matter. Atmos. Meas. Tech. 15, 561–572. https://doi.org/10.5194/amt-15-561-2022.
Karamfilova, E., 2022. Revision of the EU ambient air quality directives 1–12. https://environment.ec.europa.eu/.
Karanasiou, A., Minguillón, M.C., Viana, M., Alastuey, A., Putaud, J.-P., Maenhaut, W., Panteliadis, P., Močnik, G., Favez, O., Kuhlbusch, T.A.J., 2015. Thermal-optical analysis for the measurement of elemental carbon (EC) and organic carbon (OC) in ambient air a literature review. Atmos. Meas. Tech. Discuss 8, 9649–9712. https://doi.org/10.5194/amtd-8-9649-2015.
Karanasiou, A., Panteliadis, P., Perez, N., Minguillón, M.C., Pandolfi, M., Titos, G., Viana, M., Moreno, T., Querol, X., Alastuey, A., 2020. Evaluation of the semi-continuous OCEC analyzer performance with the EUSAAR2 protocol. Sci. Total Environ. 747 https://doi.org/10.1016/j.scitotenv.2020.141266.
Knox, A., Evans, G.J., Brook, J.R., Yao, X., Jeong, C.H., Godri, K.J., Sabaliauskas, K., Slowik, J.G., 2009. Mass absorption cross-section of ambient black carbon aerosol in relation to chemical age. Aerosol Sci. Technol. 43, 522–532. https://doi.org/10.1080/02786820902777207.
Kondo, Y., Sahu, L., Kuwata, M., Miyazaki, Y., Takegawa, N., Moteki, N., Imaru, J., Han, S., Nakayama, T., Oanh, N.T.K., Hu, M., Kim, Y.J., Kita, K., 2009. Stabilization of the mass absorption cross section of black carbon for filter-based absorption photometry by the use of a heated inlet. Aerosol Sci. Technol. 43, 741–756. https://doi.org/10.1080/02786820902889879.
Kuula, J., Timonen, H., Niemi, J.V., Manninen, H.E., Rönkkö, T., Hussein, T., Fung, P.L., Tarkoma, S., Laakso, M., Saukko, E., Ovaska, A., Kulmala, M., Karppinen, A., Johansson, L., Petäjä, T., 2022. Opinion: insights into updating ambient air quality directive 2008/50/EC. Atmos. Chem. Phys. 22, 4801–4808. https://doi.org/10.5194/acp-22-4801-2022.
Laborde, M., Crippa, M., Tritscher, T., Jurányi, Z., Decarlo, P.F., Temime-Roussel, B., Marchand, N., Eckhardt, S., Stohl, A., Baltensperger, U., Prévôt, A.S.H., Weingartner, E., Gysel, M., 2013. Black carbon physical properties and mixing state in the European megacity Paris. Atmos. Chem. Phys. 13, 5831–5856. https://doi.org/10.5194/acp-13-5831-2013.
Laj, P., Bigi, A., Rose, C., Andrews, E., Lund Myhre, C., Collaud Coen, M., Lin, Y., Wiedensohler, A., Schulz, M., A. Ogren, J., Fiebig, M., Gliß, J., Mortier, A., Pandolfi, M., Petäja, T., Kim, S.W., Aas, W., Putaud, J.P., Mayol-Bracero, O., Keywood, M., Labrador, L., Aalto, P., Ahlberg, E., Alados Arboledas, L., Alastuey, A., Andrade, M., Artinano, B., Ausmeel, S., Arsov, T., Asmi, E., Backman, J., Baltensperger, U., Bastian, S., Bath, O., Paul Beukes, J., T. Brem, B., Bukowiecki, N., Conil, S., Couret, C., Day, D., Dayantolis, W., Degorska, A., Eleftheriadis, K., Fetfatzis, P., Favez, O., Flentje, H., I. Gini, M., Gregorič, A., Gysel-Beer, M., Gannet Hallar, A., Hand, J.,

Hoffer, A., Hueglin, C., K. Hooda, R., Hyvärinen, A., Kalapov, I., Kalivitis, N., Kasper-Giebl, A., Eun Kim, J., Kouvarakis, G., Kranjc, I., Krejci, R., Kulmala, M., Labuschagne, C., Lee, H.J., Lihavainen, H., Lin, N.H., Löschau, G., Luoma, K., Marinoni, A., Martins Dos Santos, S., Meinhardt, F., Merkel, M., Metzger, J.M., Mihalopoulos, N., Anh Nguyen, N., Ondracek, J., Pérez, N., Rita Perrone, M., Pichon, J.M., Picard, D., Pichon, J.M., Pont, V., Prats, N., Prenni, A., Reisen, F., Romano, S., Sellegri, K., Sharma, S., Schauer, G., Sheridan, P., Patrick Sherman, J., Schütze, M., Schwerin, A., Sohmer, R., Sorribas, M., Steinbacher, M., Sun, J., Titos, G., Toczko, B., Tuch, T., Tulet, P., Tunved, P., Vakkari, V., Velarde, F., Velasquez, P., Villani, P., Vratolis, S., Wang, S.H., Weinhold, K., Weller, R., Yela, M., Yus-Diez, J., Zdimal, V., Zieger, P., Zikova, N., 2020. A global analysis of climate-relevant aerosol properties retrieved from the network of Global Atmosphere Watch (GAW) near-surface observatories. Atmos. Meas. Tech. 13, 4353–4392. doi: 10.5194/amt-13-4353-2020.

Liu, F., Yon, J., Fuentes, A., Lobo, P., Smallwood, G.J., Corbin, J.C., 2020. Review of recent literature on the light absorption properties of black carbon: refractive index, mass absorption cross section, and absorption function. Aerosol Sci. Technol. 54, 33–51. https://doi.org/10.1080/02786826.2019.1676878.

Luoma, K., Niemi, J.V., Aurela, M., Lun Fung, P., Helin, A., Hussein, T., Kangas, L., Kousa, A., Rönkkö, T., Timonen, H., Virkkula, A., Peťäja, T., 2021. Spatiotemporal variation and trends in equivalent black carbon in the Helsinki metropolitan area in Finland. Atmos. Chem. Phys. 21, 1173–1189. https://doi.org/10.5194/acp-21-1173-2021.

Lyamani, H., Olmo, F.J., Foyo, I., Alados-Arboledas, L., 2011. Black carbon aerosols over an urban area in South-Eastern Spain: changes detected after the 2008 economic crisis. Atmos. Environ. 45, 6423–6432. https://doi.org/10.1016/j.atmosenv.2011.07.063.

Masiol, M., Squizzato, S., Chalupa, D.C., Utell, M.J., Rich, D.Q., Hopke, P.K., 2018. Long-term trends in submicron particle concentrations in a metropolitan area of the northeastern United States. Sci. Total Environ. 633, 59–70. https://doi.org/10.1016/j.scitotenv.2018.03.151.

Masiol, M., Squizzato, S., Rich, D.Q., Hopke, P.K., 2019. Long-term trends (2005–2016) of source apportioned PM2.5 across New York State. Atmos. Environ. 201, 110–120. https://doi.org/10.1016/j.atmosenv.2018.12.038.

Mbengue, S., Serfozo, N., Schwarz, J., Holoubek, I., Ziková, N., Šmejkalová, A.H., Holoubek, I., 2020. Characterization of equivalent black carbon at a regional background site in Central Europe: variability and source apportionment☆. Environ. Pollut. 260 https://doi.org/10.1016/j.envpol.2019.113771.

Mbengue, S., Zikova, N., Schwarz, J., Vodička, P., Šmejkalová, A.H., Holoubek, I., 2021. Mass absorption cross-section and absorption enhancement from long term black and elemental carbon measurements: a rural background station in Central Europe. Sci. Total Environ. 794 https://doi.org/10.1016/j.scitotenv.2021.148365.

Moschos, V., Gysel-Beer, M., Modini, R.L., Corbin, J.C., Massabò, D., Costa, C., Danelli, S. G., Vlachou, A., Daellenbach, K.R., Szidat, S., Prati, P., Prévôt, A.S.H., Baltensperger, U., El Haddad, I., 2021. Source-specific light absorption by carbonaceous components in the complex aerosol matrix from yearly filter-based measurements. Atmos. Chem. Phys. 21, 12809–12833. https://doi.org/10.5194/acp-21-12809-2021.

Mousavi, A., Sowlat, M.H., Lovett, C., Rauber, M., Szidat, S., Bo, R., Borgini, A., Marco, C. D., Ruprecht, A.A., Sioutas, C., Boffi, R., Borgini, A., De Marco, C., Ruprecht, A.A., Sioutas, C., Bo, R., Borgini, A., Marco, C.D., Ruprecht, A.A., Sioutas, C., 2019. Source apportionment of black carbon (BC) from fossil fuel and biomass burning in metropolitan Milan, Italy. Atmos. Environ. 203, 252–261. https://doi.org/10.1016/j.atmosenv.2019.02.009.

Müller, T., Fiebig, M., 2018a. ACTRIS In Situ Aerosol: Guidelines for Manual QC of AE33 absorption photometer data. https://www.actris-ecac.eu/.

Müller, T., Fiebig, M., 2018b. ACTRIS In Situ Aerosol: Guidelines for Manual QC of MAAP (Multiangle Absorption Photometer) data. https://www.actris-ecac.eu/.

Müller, T., Henzing, J.S., De Leeuw, G., Wiedensohler, A., Alastuey, A., Angelov, H., Bizjak, M., Collaud Coen, M., Engström, J.E., Gruening, C., Hillamo, R., Hoffer, A., Imre, K., Ivanow, P., Jennings, G., Sun, J.Y., Kalivitis, N., Karlsson, H., Komppula, M., Laj, P., Li, S.M., Lunder, C., Marinoni, A., Martins Dos Santos, S., Moerman, M., Nowak, A., Ogren, J.A., Petzold, A., Pichon, J.M., Rodriquez, S., Sharma, S., Sheridan, P.J., Teinilä, K., Tuch, T., Viana, M., Virkkula, A., Weingartner, E., Wilhelm, R., Wang, Y.Q., 2011. Characterization and intercomparison of aerosol absorption photometers: result of two intercomparison workshops. Atmos. Meas. Tech. 4, 245–268. https://doi.org/10.5194/amt-4-245-2011.

Nordmann, S., Birmili, W., Weinhold, K., Müller, K., Spindler, G., Wiedensohler, A., 2013. Measurements of the mass absorption cross section of atmospheric soot particles using Raman spectroscopy. J. Geophys. Res. Atmos. 118, 12075–12085. https://doi.org/10.1002/2013JD020021.

Olson, M.R., Garcia, M.V., Robinson, M.A., Rooy, P.V., Dietenberger, M.A., Bergin, M., Schauer, J.J., 2015. Investigation of black and brown carbon multiple-wavelength-dependent light absorption from biomass and fossil fuel combustion source emissions. J. Geophys. Res. Atmos. 6682–6697. https://doi.org/10.1002/2014JD022970.

Pandolfi, M., Cusack, M., Alastuey, A., Querol, X., 2011. Variability of aerosol optical properties in the Western Mediterranean Basin. Atmos. Chem. Phys. 8189–8203. https://doi.org/10.5194/acp-11-8189-2011.

Pandolfi, M., Ripoll, A., Querol, X., Alastuey, A., 2014a. Climatology of aerosol optical properties and black carbon mass absorption cross section at a remote high-altitude site in the western Mediterranean Basin. Atmos. Chem. Phys. 14, 6443–6460. https://doi.org/10.5194/acp-14-6443-2014.

Pandolfi, M., Tobias, A., Alastuey, A., Sunyer, J., Schwartz, J., Lorente, J., Pey, J., Querol, X., 2014b. Effect of atmospheric mixing layer depth variations on urban air quality and daily mortality during Saharan dust outbreaks. Sci. Total Environ. 495, 283–289. https://doi.org/10.1016/j.scitotenv.2014.07.004.

Pandolfi, M., Alados-arboledas, L., Alastuey, A., Andrade, M., Angelov, C., 2018. A European aerosol phenomenology – 6: scattering properties of atmospheric aerosol particles from 28 ACTRIS sites. Atmos. Chem. Phys. 18, 7877–7911. https://doi.org/10.5194/acp-18-7877-2018.

Pandolfi, M., Mooibroek, D., Hopke, P., Van Pinxteren, D., Querol, X., Herrmann, H., Alastuey, A., Favez, O., Hüglin, C., Perdrix, E., Riffault, V., Sauvage, S., Van Der Swaluw, E., Tarasova, O., Colette, A., 2020. Long-range and local air pollution: what can we learn from chemical speciation of particulate matter at paired sites? Atmos. Chem. Phys. 20, 409–429. https://doi.org/10.5194/acp-20-409-2020.

Petzold, A., Schloesser, H., Sheridan, P.J., Arnott, W.P., Ogren, J.A., Virkkula, A., 2005. Evaluation of multiangle absorption photometry for measuring aerosol light absorption. Aerosol Sci. Technol. 39, 40–51. https://doi.org/10.1080/027868290901945.

Petzold, A., Ogren, J.A., Fiebig, M., Laj, P., Li, S.M., Baltensperger, U., Holzer-Popp, T., Kinne, S., Pappalardo, G., Sugimoto, N., Wehrli, C., Wiedensohler, A., Zhang, X.Y., 2013. Recommendations for reporting black carbon measurements. Atmos. Chem. Phys. 13, 8365–8379. https://doi.org/10.5194/acp-13-8365-2013.

Petzold, A., Schönlinner, M., 2004. Multi-angle absorption photometry - a new method for the measurement of aerosol light absorption and atmospheric black carbon. J. Aerosol Sci. 35, 421–441. https://doi.org/10.1016/j.jaerosci.2003.09.005.

Pileci, R.E., Modini, R.L., Bertò, M., Yuan, J., Corbin, J.C., Marinoni, A., Henzing, B., Moerman, M.M., Putaud, J.P., Spindler, G., Wehner, B., Müller, T., Tuch, T., Trentini, A., Zanatta, M., Baltensperger, U., Gysel-Beer, M., 2021. Comparison of co-located refractory black carbon (rBC) and elemental carbon (EC) mass concentration measurements during field campaigns at several European sites. Atmos. Meas. Tech. 14, 1379–1403. https://doi.org/10.5194/amt-14-1379-2021.

Presler-Jur, P., Doraiswamy, P., Hammond, O., Rice, J., 2017. An evaluation of mass absorption cross-section for optical carbon analysis on Teflon filter media. J. Air Waste Manag. Assoc. 67, 1213–1228. https://doi.org/10.1080/10962247.2017.1310148.

Proposal for a Directive of the European Parliament and of the Council on ambient air quality and cleaner air for Europe (recast), Mandate for negotiations with the European Parliament, Brussels, 9 November 2023, Council of the European Union.

Putaud, J.P., Cavalli, F., Santos, S.M., Acqua, A.D., 2014. Long-term trends in aerosol optical characteristics in the Po Valley , Italy 9129–9136. doi: 10.5194/acp-14-9129-2014.

Querol, X., Pérez, N., Reche, C., Ealo, M., Ripoll, A., Tur, J., Pandolfi, M., Pey, J., Salvador, P., Moreno, T., Alastuey, A., 2019. African dust and air quality over Spain: is it only dust that matters? Sci. Total Environ. 686, 737–752. https://doi.org/10.1016/j.scitotenv.2019.05.349.

Ram, K., Sarin, M.M., 2009. Absorption coefficient and site-specific mass absorption efficiency of elemental carbon in aerosols over urban, rural, and high-altitude sites in India. Environ. Sci. Technol. 43, 8233–8239. https://doi.org/10.1021/es9011542.

Rattigan, O.V., Civerolo, K., Doraiswamy, P., Felton, H.D., Hopke, P.K., 2013. Long term black carbon measurements at two urban locations in New York. Aerosol Air Qual. Res. 13, 1181–1196. https://doi.org/10.4209/aaqr.2013.02.0060.

Rigler, M., Drinovec, L., Lavri, G., Vlachou, A., Prevot, A.S.H., Luc Jaffrezo, J., Stavroulas, I., Sciare, J., Burger, J., Kranjc, I., Turšič, J., Hansen, D.A., Mocnik, G., 2020. The new instrument using a TC-BC (total carbon-black carbon) method for the online measurement of carbonaceous aerosols. Atmos. Meas. Tech. 13, 4333–4351. https://doi.org/10.5194/amt-13-4333-2020.

Ripoll, A., Minguillón, M.C., Pey, J., Jimenez, J.L., Day, D.A., Sosedova, Y., Canonaco, F., Prévôt, A.S.H., Querol, X., Alastuey, A., 2015. Long-term real-time chemical characterization of submicron aerosols at Montsec (southern Pyrenees, 1570 m a.s. l.). Atmos. Chem. Phys. 15, 2935–2951. https://doi.org/10.5194/acp-15-2935-2015.

RI-URBANS, 2020. Research Infrastructures Services Reinforcing Air Quality Monitoring Capacities in European Urban & Industrial AreaS (RI-URBANS), Technical annex, Horizon 2020, LC-GD-9-1-2020, Work programme H2020-2018-2020. https://riurbans.eu/.

Salako, G.O., Hopke, P.K., Cohen, D.D., Begum, B.A., Biswas, S.K., Pandit, G.G., Chung, Y.S., Rahman, S.A., Hamzah, M.S., Davy, P., Markwitz, A., Shagjjamba, D., Lodoysamba, S., Wimolwattanapun, W., Bunprapob, S., 2012. Exploring the variation between EC and BC in a variety of locations. Aerosol Air Qual. Res. 12, 1–7. https://doi.org/10.4209/aaqr.2011.09.0150.

Sandrini, S., Fuzzi, S., Piazzalunga, A., Prati, P., Bonasoni, P., Cavalli, F., Bove, M.C., Calvello, M., Cappelletti, D., Colombi, C., Contini, D., de Gennaro, G., Di Gilio, A., Fermo, P., Ferrero, L., Gianelle, V., Giugliano, M., Ielpo, P., Lonati, G., Marinoni, A., Massabò, D., Molteni, U., Moroni, B., Pavese, G., Perrino, C., Perrone, M.R.G., Perrone, M.R.G., Putaud, J.P., Sargolini, T., Vecchi, R., Gilardoni, S., 2014. Spatial and seasonal variability of carbonaceous aerosol across Italy. Atmos. Environ. 99, 587–598. https://doi.org/10.1016/j.atmosenv.2014.10.032.

Savadkoohi, M., Pandolfi, M., Reche, C., Niemi, J.V., Mooibroek, D., Titos, G., Green, D. C., Tremper, A.H., Hueglin, C., Coz, E., Liakakou, E., Mihalopoulos, N., Stavroulas, I., Alados-arboledas, L., Beddows, D., Brito, J.F.D., Bastian, S., Baudic, A., Colombi, C., Costabile, F., Estell, V., Matos, V., Gaag, E.V., Silvergren, S., Petit, J., Putaud, J., Rattigan, O.V., Timonen, H., Tuch, T., Merkel, M., Weinhold, K., Vratolis, S., Vasilescu, J., Favez, O., Harrison, R.M., Laj, P., Wiedensohler, A., Hopke, P.K., Pet, T., Querol, X., 2023. The variability of mass concentrations and source apportionment analysis of equivalent black carbon across urban Europe. Environ. Int. J. 178 https://doi.org/10.1016/j.envint.2023.108081.

Schmid, H., Laskus, L., Jürgen Abraham, H., Baltensperger, U., Lavanchy, V., Bizjak, M., Burba, P., Cachier, H., Crow, D., Chow, J., Gnauk, T., Even, A., Ten Brink, H.M., Giesen, K.P., Hitzenberger, R., Hueglin, C., Maenhaut, W., Pio, C., Carvalho, A.,

Putaud, J.P., Toom-Sauntry, D., Puxbaum, H., 2001. Results of the "carbon conference" international aerosol carbon round robin test stage I. Atmos. Environ. 35, 2111–2121. https://doi.org/10.1016/S1352-2310(00)00493-3.
Snyder, D.C., Schauer, J.J., 2007. An inter-comparison of two black carbon aerosol instruments and a semi-continuous elemental carbon instrument in the urban environment. Aerosol Sci. Technol. 41, 463–474. https://doi.org/10.1080/02786820701222819.
Srivastava, P., Naja, M., Seshadri, T.R., Joshi, H., Dumka, U.C., Gogoi, M.M., Babu, S.S., 2022. Implications of site-specific mass absorption cross-section (MAC) to black carbon observations at a high-altitude site in the central Himalaya. Asia-Pacific J. Atmos. Sci. 58, 83–96. https://doi.org/10.1007/s13143-021-00241-6.
STANBC. Standardisation of Black Carbon Aerosol metrics for air quality and climate modelling. https://stanbc.com.
Sun, J., Birmili, W., Hermann, M., Tuch, T., Weinhold, K., Spindler, G., Schladitz, A., Bastian, S., Löschau, G., Cyrys, J., Gu, J., Flentje, H., Briel, B., Asbach, C., Kaminski, H., Ries, L., Sohmer, R., Gerwig, H., Wirtz, K., Meinhardt, F., Schwerin, A., Bath, O., Ma, N., Wiedensohler, A., 2019. Variability of black carbon mass concentrations, sub-micrometer particle number concentrations and size distributions: results of the German ultrafine aerosol network ranging from city street to high Alpine locations. Atmos. Environ. 202, 256–268. https://doi.org/10.1016/j.atmosenv.2018.12.029.
Sun, J., Birmili, W., Hermann, M., Tuch, T., Weinhold, K., Merkel, M., Rasch, F., Müller, T., Schladitz, A., Bastian, S., Löschau, G., Cyrys, J., Gu, J., Flentje, H., Briel, B., Asbach, C., Kaminski, H., Ries, L., Sohmer, R., Gerwig, H., Wirtz, K., Meinhardt, F., Schwerin, A., Bath, O., Ma, N., Wiedensohler, A., 2020. Decreasing trends of particle number and black carbon mass concentrations at 16 observational sites in Germany from 2009 to 2018. Atmos. Chem. Phys. 20, 7049–7068. https://doi.org/10.5194/acp-20-7049-2020.
Titos, G., del Águila, A., Cazorla, A., Lyamani, H., Casquero-Vera, J.A., Colombi, C., Cuccia, E., Gianelle, V., Močnik, G., Alastuey, A., Olmo, F.J., Alados-Arboledas, L., 2017. Spatial and temporal variability of carbonaceous aerosols: assessing the impact of biomass burning in the urban environment. Sci. Total Environ. 578, 613–625. https://doi.org/10.1016/j.scitotenv.2016.11.007.
Trechera, P., Garcia-Marlès, M., Liu, X., Reche, C., Pérez, N., Savadkoohi, M., Beddows, D., Salma, I., Vörösmarty, M., Casans, A., Casquero-Vera, J.A., Hueglin, C., Marchand, N., Chazeau, B., Gille, G., Kalkavouras, P., Mihalopoulos, N., Ondracek, J., Zikova, N., Niemi, J.V., Manninen, H.E., Green, D.C., Tremper, A.H., Norman, M., Vratolis, S., Eleftheriadis, K., Gómez-Moreno, F.J., Alonso-Blanco, E., Gerwig, H., Wiedensohler, A., Weinhold, K., Merkel, M., Bastian, S., Petit, J.E., Favez, O., Crumeyrolle, S., Ferlay, N., Martins Dos Santos, S., Putaud, J.P., Timonen, H., Lampilahti, J., Asbach, C., Wolf, C., Kaminski, H., Altug, H., Hoffmann, B., Rich, D.Q., Pandolfi, M., Harrison, R.M., Hopke, P.K., Petäjä, T., Alastuey, A., Querol, X., 2023. Phenomenology of ultrafine particle concentrations and size distribution across urban Europe. Environ. Int. 172, 107744 https://doi.org/10.1016/j.envint.2023.107744.
Turner, J.R., Hansen, A.D., Allen, G.A., 2007. Methodologies to compensate for optical saturation and scattering in Aethalometer™ black carbon measurements. Air Waste Manag. Assoc. - Symp. Air Qual. Meas. Methods Technol. 2007 165 CP, 20–24.
Ushey, K., 2022. Package ' RcppRoll ' 1–5. https://CRAN.R-project.org/package=RcppRoll.
Valentini, S., Bernardoni, V., Bolzacchini, E., Ciniglia, D., Ferrero, L., Forello, A.C., Massabó, D., Pandolfi, M., Prati, P., Soldan, F., Valli, G., Yus-Díez, J., Alastuey, A., Vecchi, R., 2021. Applicability of benchtop multi-wavelength polar photometers to off-line measurements of the Multi-Angle Absorption Photometer (MAAP) samples. J. Aerosol Sci. 152, 1–13. https://doi.org/10.1016/j.jaerosci.2020.105701.
van Drooge, B.L., Garatachea, R., Reche, C., Titos, G., Alastuey, A., Lyamani, H., Alados-Arboledas, L., Querol, X., Grimalt, J.O., 2022. Primary and secondary organic winter aerosols in Mediterranean cities under different mixing layer conditions (Barcelona and Granada). Environ. Sci. Pollut. Res. 29, 36255–36272. https://doi.org/10.1007/s11356-021-16366-0.
Varga, G., Újvári, G., Kovács, J., 2014. Spatiotemporal patterns of Saharan dust outbreaks in the Mediterranean Basin. Aeolian Res. 15, 151–160. https://doi.org/10.1016/j.aeolia.2014.06.005.
Via, M., Minguillón, M.C., Reche, C., Querol, X., Alastuey, A., 2021. Increase in secondary organic aerosol in an urban environment. Atmos. Chem. Phys. 21, 8323–8339. https://doi.org/10.5194/acp-21-8323-2021.
Virkkula, A., Mäkelä, T., Hillamo, R., Yli-Tuomi, T., Hirsikko, A., Hämeri, K., Koponen, I. K., 2007. A simple procedure for correcting loading effects of aethalometer data. J. Air Waste Manag. Assoc. 57, 1214–1222. https://doi.org/10.3155/1047-3289.57.10.1214.
Vodička, P., Kawamura, K., Schwarz, J., Ždímal, V., 2022. Seasonal changes in stable carbon isotopic composition in the bulk aerosol and gas phases at a suburban site in Prague. Sci. Total Environ. 803 https://doi.org/10.1016/j.scitotenv.2021.149767.
Vodička, P., Kawamura, K., Schwarz, J., Ždímal, V., 2023. A year-round observation of δ13C of dicarboxylic acids and related compounds in fine aerosols: implications from Central European background site. Chemosphere 337. https://doi.org/10.1016/j.chemosphere.2023.139393.
Wang, Y., Hopke, P.K., Rattigan, O.V., Chalupa, D.C., Utell, M.J., 2012. Multiple-year black carbon measurements and source apportionment using Delta-C in Rochester, New York. J. Air Waste Manag. Assoc. 62, 880–887. https://doi.org/10.1080/10962247.2012.671792.
Wang, Y., Liu, S., Shi, P., Li, Y., Mu, C., Du, K., 2013. Temporal variation of mass absorption efficiency of black carbon at urban and suburban locations. Aerosol Air Qual. Res. 13, 275–286. https://doi.org/10.4209/aaqr.2012.05.0125.
Weingartner, E., Saathoff, H., Schnaiter, M., Streit, N., Bitnar, B., Baltensperger, U., 2003. Absorption of light by soot particles: determination of the absorption coefficient by means of aethalometers. J. Aerosol Sci. 34, 1445–1463. https://doi.org/10.1016/S0021-8502(03)00359-8.
WHO, 2021. WHO global air quality guidelines. Particulate matter (PM2.5 and PM10), ozone, nitrogen dioxide, sulfur dioxide and carbon monoxide. World Health Organization, Geneva; 2021. Licence: CC BY-NC-SA 3.0 IGO.
Wu, B., Xuan, K., Zhang, X., Shen, X., Li, X., Zhou, Q., Cao, X., Zhang, H., Yao, Z., 2021. Mass absorption cross-section of black carbon from residential biofuel stoves and diesel trucks based on real-world measurements. Sci. Total Environ. 784, 147225 https://doi.org/10.1016/j.scitotenv.2021.147225.
Yuan, J., Lewis Modini, R., Zanatta, M., Herber, A.B., Müller, T., Wehner, B., Poulain, L., Tuch, T., Baltensperger, U., Gysel-Beer, M., 2021. Variability in the mass absorption cross section of black carbon (BC) aerosols is driven by BC internal mixing state at a central European background site (Melpitz, Germany) in winter. Atmos. Chem. Phys. 21, 635–655. https://doi.org/10.5194/acp-21-635-2021.
Yus-Díez, J., Bernardoni, V., Močnik, G., Alastuey, A., Ciniglia, D., Ivančič, M., Querol, X., Perez, N., Reche, C., Rigler, M., Vecchi, R., Valentini, S., Pandolfi, M., 2021. Determination of the multiple-scattering correction factor and its cross-sensitivity to scattering and wavelength dependence for different AE33 Aethalometer filter tapes: a multi-instrumental approach. Atmos. Meas. Tech. Discuss. 14, 6335–6355. https://doi.org/10.5194/amt-2021-46.
Yus-díez, J., Via, M., Alastuey, A., Karanasiou, A., Minguillón, M.C., Perez, N., Querol, X., Reche, C., Ivaň, M., 2022. Absorption enhancement of black carbon particles in a Mediterranean city and countryside: effect of particulate matter chemistry, ageing and trend. Atmos. Chem. Phys. 22, 8439–8456. https://doi.org/10.5194/acp-22-8439-2022.
Zanatta, M., Gysel, M., Bukowiecki, N., Müller, T., Weingartner, E., Areskoug, H., Fiebig, M., Yttri, K.E., Mihalopoulos, N., Kouvarakis, G., Beddows, D., Harrison, R. M., Cavalli, F., Putaud, J.P., Spindler, G., Wiedensohler, A., Alastuey, A., Pandolfi, M., Sellegri, K., Swietlicki, E., Jaffrezo, J.L., Baltensperger, U., Laj, P., 2016. A European aerosol phenomenology-5: climatology of black carbon optical properties at 9 regional background sites across Europe. Atmos. Environ. 145, 346–364. https://doi.org/10.1016/j.atmosenv.2016.09.035.
Zeileis, A., Grothendieck, G., 2005. Zoo: S3 infrastructure for regular and irregular time series. J. Stat. Softw. 14 https://doi.org/10.18637/jss.v014.i06.
Zhang, Y., Albinet, A., Petit, J.E., Jacob, V., Chevrier, F., Gille, G., Pontet, S., Chrétien, E., Dominik-Sègue, M., Levigoureux, G., Močnik, G., Gros, V., Jaffrezo, J.L., Favez, O., 2020. Substantial brown carbon emissions from wintertime residential wood burning over France. Sci. Total Environ. 743 https://doi.org/10.1016/j.scitotenv.2020.140752.
Zhang, Y., Favez, O., Canonaco, F., Liu, D., Prévôt, A.S.H., Gros, V., Albinet, A., 2018. Evidence of major secondary organic aerosol contribution to lensing effect black carbon absorption enhancement. doi: 10.1038/s41612-018-0056-2.
Zhang, Y., Favez, O., Petit, J.E., Canonaco, F., Truong, F., Bonnaire, N., Crenn, V., Amodeo, T., Prévôt, A.S.H., Sciare, J., Gros, V., Albinet, A., 2019. Six-year source apportionment of submicron organic aerosols from near-continuous highly time-resolved measurements at SIRTA (Paris area, France). Atmos. Chem. Phys. 19, 14755–14776. https://doi.org/10.5194/acp-19-14755-2019.
Zhao, W., Tan, W., Zhao, G., Shen, C., Yu, Y., Zhao, C., 2021. Determination of equivalent black carbon mass concentration from aerosol light absorption using variable mass absorption cross section. Atmos. Meas. Tech. 14, 1319–1331. https://doi.org/10.5194/amt-14-1319-2021.
Zíková, N., Vodička, P., Ludwig, W., Hitzenberger, R., Schwarz, J., 2016. On the use of the field Sunset semi-continuous analyzer to measure equivalent black carbon concentrations. Aerosol Sci. Technol. 50, 284–296. https://doi.org/10.1080/02786826.2016.1146819.
Zotter, P., Herich, H., Gysel, M., El-Haddad, I., Zhang, Y., Mocnik, G., Hüglin, C., Baltensperger, U., Szidat, S., Prévôt, A.S.H., 2017. Evaluation of the absorption Ångström exponents for traffic and wood burning in the Aethalometer-based source apportionment using radiocarbon measurements of ambient aerosol. Atmos. Chem. Phys. 17, 4229–4249. https://doi.org/10.5194/acp-17-4229-2017.